DMD Fast Forward. Published on July 2, 2013 as doi:10.1124/dmd.113.052084

Biotransformation of a Novel Positive Allosteric Modulator of Metabotropic Glutamate Receptor Subtype 5 Contributes to Seizure-Like Adverse Events in Rats Involving a Receptor Agonism-Dependent Mechanism

Thomas M. Bridges, Jerri M. Rook, Meredith J. Noetzel, Ryan D. Morrison, Ya Zhou, Rocco D. Gogliotti, Paige N. Vinson, Zixiu Xiang, Carrie K. Jones, Colleen M. Niswender, Craig W. Lindsley, Shaun R. Stauffer, P. Jeffrey Conn, J. Scott Daniels

Drug Metabolism and Pharmacokinetics (T.M.B., R.D.M., J.S.D.), Molecular Pharmacology (J.M.R., M.J.N., P.N.V., Z.X., C.M.N., P.J.C.), Behavioral Pharmacology (C.K.J.), Medicinal Chemistry (Y.Z., R.D.G., C.W.L., S.R.S.), Vanderbilt Center for Neuroscience Drug Discovery, Vanderbilt University Medical Center, Nashville, TN 37232, USA

DMD Fast Forward. Published on July 2, 2013 as DOI: 10.1124/dmd.113.052084
This article has not been copyedited and formatted. The final version may differ from this version.

***Running Title*:** biotransformation of $mGlu_5$ PAM to active agonist metabolite

***Corresponding Author*:** Dr. J. Scott Daniels, Department of Pharmacology, Vanderbilt Center for Neuroscience Drug Discovery, Vanderbilt University Medical Center, Nashville, TN 37232-6600, USA. Email: scott.daniels@vanderbilt.edu; Phone: 615-322-0673; Fax: 615-875-3375

Number of Text Pages: 36
Number of Tables: 1
Number of Figures: 8
Number of References: 28
Number of words in Abstract: 249
Number of words in Introduction: 750
Number of words in Discussion: 1132

***Abbreviations*:** $mGlu_5$, metabotropic glutamate receptor subtype 5; PAM, positive allosteric modulator; IVIVC, *in vitro-in vivo* correlation; HLM or RLM, human liver microsomes or rat liver microsomes; S9, subcellular fraction containing microsomes and cytosol; CL_{int}, intrinsic clearance; CL_{hep}, predicted hepatic clearance; 1-ABT, 1-aminobenzotriazole; COSY, correlation spectroscopy; HMBC, heteronuclear multiple bond correlation spectroscopy; HSQC, heteronuclear spin-quantum correlation spectroscopy.

DMD Fast Forward. Published on July 2, 2013 as DOI: 10.1124/dmd.113.052084
This article has not been copyedited and formatted. The final version may differ from this version.

Abstract:

Activation of metabotropic glutamate receptor subtype 5 ($mGlu_5$) represents a novel strategy for therapeutic intervention into multiple central nervous system (CNS) disorders including schizophrenia. Recently, a number of positive allosteric modulators (PAMs) of $mGlu_5$ have been discovered to exhibit *in vivo* efficacy in rodent models of psychosis, including PAMs possessing varying degrees of agonist activity (ago-PAMs) as well as PAMs devoid of agonist activity. However, previous studies revealed that ago-PAMs can induce seizure activity and behavioral convulsions, whereas pure $mGlu_5$ PAMs do not induce these adverse effects. We recently identified a potent and selective $mGlu_5$ PAM, VU0403602, which was efficacious in reversing amphetamine-induced hyperlocomotion in rats. The compound also induced time-dependent seizure activity that was blocked by co-administration of the $mGlu_5$ antagonist, 2-methyl-6-(phenylethynyl) pyridine (MPEP). Consistent with potential adverse effects induced by ago-PAMs, we found that VU0403602 had significant allosteric agonist activity. Interestingly, inhibition of VU0403602 metabolism *in vivo* by a pan P450-inactivator completely protected rats from induction of seizures. P450-mediated biotransformation of VU0403602 was discovered to produce another potent ago-PAM metabolite-ligand (**M1**) of $mGlu_5$. Electrophysiological studies in rat hippocampal slices confirmed agonist activity of both **M1** and VU0403602 and revealed that **M1** can induce epileptiform activity in a manner consistent with its pro-convulsant behavioral effects. Furthermore, unbound brain exposure of **M1** was similar to that of the parent compound VU0403602. These findings indicate that biotransformation of $mGlu_5$ PAMs to active metabolite-ligands may contribute to the epileptogenesis observed following *in vivo* administration of this class of allosteric receptor modulators.

DMD Fast Forward. Published on July 2, 2013 as DOI: 10.1124/dmd.113.052084
This article has not been copyedited and formatted. The final version may differ from this version.

Introduction:

Initiated largely by the *N*-methyl-D-aspartate (NMDA) receptor hypofunction hypothesis, we and others have identified $mGlu_5$ as a potential means for therapeutic intervention in central nervous system (CNS) disorders such as schizophrenia(Olney et al., 1999; Tsai and Coyle, 2002; Conn et al., 2009; Marek et al., 2010; Gregory et al., 2011; Vinson and Conn, 2012). To this end, we have successfully identified potent and selective positive allosteric modulators (PAMs) of $mGlu_5$ that are orally active in rodent models of psychosis and in various cognitive paradigms(Hammond et al., 2010; Rodriguez et al., 2010; Williams et al., 2011). Recently, we described several PAMs possessing intrinsic agonist activity that stimulate glutamate-independent signaling(Noetzel et al., 2012). Some of these agonist-PAM (ago-PAM) compounds have recently been found to induce $mGlu_5$-dependent limbic seizures similar to the adverse events (AEs) reported in rodents receiving intracerebral administration of the $mGlu_5$ agonist, dihydroxyphenylglycine (DHPG)(Tizzano et al., 1995b; Tizzano et al., 1995a; Rook et al., 2012). Moreover, results from electrophysiological experiments confirm an induction of epileptiform activity following treatment of rat hippocampal slices with $mGlu_5$ agonists; this effect was attenuated by an $mGlu_5$ antagonist(Lee et al., 2002; Zhao et al., 2004; Wong et al., 2005). Collectively, our observations are consistent with recent assertions that group I mGlu receptor activation can be a critical initiation step contributing to propagation of epileptogenic discharges in the CNS(Wong et al., 2005).

We previously reported on a group of highly selective $mGlu_5$ allosteric modulators displaying favorable pharmacokinetic (PK) properties and PAM or ago-PAM activity as determined by Ca^{2+} mobilization in recombinant cells and in cortical astrocytes(Rook et al., 2012). Importantly, electrophysiological experiments indicated that ago-PAMs such as

DMD Fast Forward. Published on July 2, 2013 as DOI: 10.1124/dmd.113.052084
This article has not been copyedited and formatted. The final version may differ from this version.

VU0424465 induced prolonged long-term depression (LTD) and increased both the amplitude and frequency of spontaneous population spikes determined by extracellular field potential recordings in rat hippocampal slices(Rook et al., 2012). However, PAMs that were devoid of intrinsic agonist activity (VU0360172 and VU0361747) did not induce epileptiform activity(Rook et al., 2012). Finally, rats receiving a systemic administration of the ago-PAM, VU0424465, experienced pronounced seizures, which were completely prevented by pretreatment with the selective $mGlu_5$ antagonist, 2-methyl-6-(phenylethynyl) pyridine (MPEP)(Rook et al., 2012).

We have observed that several $mGlu_5$ PAM chemical series contain compounds possessing diverse modes of pharmacology, including positive allosteric modulation, negative allosteric modulation (NAM), and silent allosteric modulation (SAM)(Sharma et al., 2009; Lamb et al., 2011; Lindsley, 2011; Williams et al., 2011; Wood et al., 2011). In many cases, single-atom modifications to compounds have resulted in a molecular switch that effectively converts PAMs to NAMs or ago-PAMs. This propensity for pharmacological 'mode-switching' represents a barrier to the optimization of $mGlu_5$ allosteric modulators due to the range of drug metabolizing enzymes (DMEs) that are capable of introducing subtle single atom oxidations to PAMs. Biotransformation of a PAM could result in the formation of active metabolites capable of (1) silencing the effect (SAM) of the parent compound, (2) activating the receptor in the absence of glutamate (ago-PAMs), or (3) reversing the allosteric modulation (NAM) of the parent PAM *in vivo*.

Herein, we describe the *in vitro* and *in vivo* pharmacology and drug metabolism and pharmacokinetic (DMPK) profile of a selective $mGlu_5$ ago-PAM, VU0403602, which induced pronounced dose- and time-dependent seizures in rats, an effect that was prevented by

DMD Fast Forward. Published on July 2, 2013 as DOI: 10.1124/dmd.113.052084
This article has not been copyedited and formatted. The final version may differ from this version.

pretreatment with MPEP. Together, these data indicated an $mGlu_5$-mediated mechanism to the neurotoxicity observed *in vivo*. Interestingly, pretreatment of rats with the pan cytochrome P450 inactivator, 1-aminobenzotriazole (ABT), effectively prevented VU0403602-induced seizures, further implicating the role of a metabolite-ligand in the onset of adverse events. *In vivo* PK studies revealed that both parent VU0403602 and the metabolite permeated the CNS of rats, and that the exposure of the metabolite was significantly reduced in rats that had been pretreated with ABT. An *in vitro* and *in vivo* appraisal of the metabolism of VU0403602 identified a principle oxidative metabolite that displayed potent ago-PAM activity. Additional studies involving systemic administration of the metabolite to rats resulted in a rapid onset of seizures, the severity of which was similar to that observed following the administration of VU0403602. Subsequent *in vitro* electrophysiological experiments indicated that the metabolite-ligand induced prolonged LTD and epileptogenic discharges in rat hippocampal slices similar to those observed with the $mGlu_5$ agonist DHPG(Tizzano et al., 1995a; Tizzano et al., 1995b; Lee et al., 2002; Zhao et al., 2004; Wong et al., 2005). Together, these findings support the hypothesis that the $mGlu_5$ ago-PAM VU0403602 undergoes P450-mediated biotransformation to an active metabolite, which itself possesses potent agonist-PAM activity and subsequently contributes to pro-convulsant behavioral effects *in vivo.*

DMD Fast Forward. Published on July 2, 2013 as DOI: 10.1124/dmd.113.052084
This article has not been copyedited and formatted. The final version may differ from this version.

Materials and Methods:

Reagents

VU0403602 (*N*-cyclobutyl-5-((3-fluorophenyl)ethynyl)picolinamide) and metabolites **M1** and **M2** (5-((3-fluorophenyl)ethynyl)-*N*-(3-hydroxycyclobutyl)picolinamide and 5-((3-fluorophenyl)ethynyl)picolinic acid, respectively) were prepared by the Medicinal Chemistry Laboratories of the Vanderbilt Center for Neuroscience Drug Discovery. Potassium phosphate, ammonium formate, formic acid, β-nicotinamide adenine dinucleotide phosphate (NADPH), magnesium chloride ($MgCl_2$), adenosine 3′-phosphate 5′-phosphosulfate lithium salt hydrate (PAPS), uridine 5'-diphosphoglucuronic acid trisodium salt (UDPGA), and 1-aminobenzotriazole (ABT) were purchased from Sigma-Aldrich Chemical Company (St. Louis, MO). Rat hepatic subcellular fractions were obtained from BD Biosciences (Woburn, MA). Rat brain S9 fractions were obtained from Celsis In Vitro Technologies (Baltimore, MD). Rat intestinal S9 fractions were obtained from Xenotech (Lenexa, KS). Dulbecco's Modified Eagle's Medium (DMEM), fetal bovine serum (FBS), and antibiotics were purchased from Invitrogen (Carlsbad, CA). DHPG was obtained from Ascent Scientific (Bristol, UK). [^{3}H]mPEPy was purchased from Perkin Elmer (Waltham, MA). 5MPEP and MPEP were synthesized as described previously.

Chemical Synthesis

General. All NMR spectra were recorded on a Bruker 400 mHz instrument. ^{1}H chemical shifts are reported in δ values in ppm downfield from TMS as the internal standard in d_3-MeOH. Data are reported as follows: chemical shift, multiplicity (s = singlet, d = doublet, t = triplet, q = quartet, br = broad, m = multiplet), integration, coupling constant (Hz). Low resolution mass

DMD Fast Forward. Published on July 2, 2013 as DOI: 10.1124/dmd.113.052084
This article has not been copyedited and formatted. The final version may differ from this version.

spectra were obtained on an Agilent 1200 series 6130 mass spectrometer. High resolution mass spectra were recorded on a Waters Q-TOF API-US. Analytical thin layer chromatography was performed on Analtech silica gel GF 250 micron plates. Analytical HPLC was performed on an HP1100 with UV detection at 214 and 254 nm along with ELSD detection, LC/MS (J-Sphere80-C18, 3.0 x 50 mm, 4.1 min gradient, 5%[0.05%TFA/CH_3CN]:95%[0.05%TFA/H_2O] to 100%[0.05%TFA/CH_3CN]. Preparative RP-HPLC purification was performed on a custom HP1100 automated purification system with collection triggered by mass detection or using a Gilson Inc. preparative UV-based system using a Phenomenex Luna C18 column (50 x 30 mm I.D., 5 μm) with an acetonitrile (unmodified)-water (0.1% TFA) custom gradient. Normal-phase silica gel preparative purification was performed using an automated Combi-flash companion from ISCO. Solvents for extraction, washing and chromatography were HPLC grade. All reagents were purchased from Aldrich Chemical Co. and were used without purification. All polymer-supported reagents were purchased from Argonaut Technologies and Biotage. Individual compound synthetic methods are contained in the Supplemental Information.

Cell Culture and Mutagenesis

HEK293A cells lines stably expressing rat $mGlu_5$ were maintained in complete DMEM supplemented with 10% FBS, 2 mM L-glutamine, 20 mM HEPES, 0.1 mM Non-Essential Amino Acids, 1 mM sodium pyruvate, antibiotic-antimycotic, and G418 (500 ug/mL; Mediatech, Manassas, VA) at 37 °C in a humidified incubator containing 5% CO_2, 95% O_2. Point mutations in rat $mGlu_5$-pCl:Neo were generated using a site-directed mutagenesis kit (Quikchange II, Agilent, Santa Clara, CA), and mutant plasmids were fully sequenced to verify the desired mutations. HEK293A cells were transfected with the mutant plasmids using Fugene6^{TM}

DMD Fast Forward. Published on July 2, 2013 as DOI: 10.1124/dmd.113.052084
This article has not been copyedited and formatted. The final version may differ from this version.

(Promega, Madison, WI), and the cells were maintained under 1 mg/mL G418 selection for 2 weeks to obtain the stable cell lines expressing these mutants. Stable polyclonal mutant rat $mGlu_5$ cells and HEK293A cells stably expressing rat $mGlu_1$ were maintained in the same media as the $mGlu_5$ wild type cells. HEK293A cells stably expressing G-protein-coupled inwardly-rectifying potassium channels (HEK293A-GIRK) and the individual group II and group III mGlu's were maintained in growth media containing 45% DMEM, 45% F-12, 10% FBS, 20 mM HEPES, 2 mM L-glutamine, antibiotic/antimycotic, non-essential amino acids, 700 μg/mL G418, and 0.6 μg/mL puromycin.

Fluorescence-Based Calcium Assays in Rat $mGlu_5$ Cells

Measurement of $mGlu_5$-mediated intracellular Ca^{2+} mobilization was performed using the Ca^{2+} sensitive dye, Fluo-4 and a Flexstation II, as described previously (Noetzel et al., 2012). HEK293A cells expressing either $mGlu_5$-wildtype or $mGlu_5$ mutants, were incubated with test compound for 60 sec prior to stimulation with glutamate. Baseline fluorescence was subtracted from peak fluorescence before normalization to the maximal peak response elicited by glutamate alone (10-100 μM). Data were transformed and fitted using GraphPad Prism 5.0 (Graph-Pad Software, Inc., San Diego, CA).

Fluorescence-Based Calcium Assays in Rat Astrocytes

Rat cortical astrocytes were plated in 384-well poly-D-lysine coated, black-walled, clear-bottomed plates (BD Falcon) in a 20 μL volume of astrocyte growth medium (AGM) at a density of approximately 15,000-20,000 cells/well and supplemented the following day with G5 diluted 1:100 in AGM. On the day of the experiment, concentration response curves (CRCs) of test

DMD Fast Forward. Published on July 2, 2013 as DOI: 10.1124/dmd.113.052084
This article has not been copyedited and formatted. The final version may differ from this version.

compounds were prepared. Stock compounds were made in DMSO at a concentration of 10 mM. CRCs were made at a 2X concentration in assay buffer (HBSS, 20 mM HEPES, 2.5 mM probenecid, pH 7.4) to achieve final concentrations in the assay that ranged from 0.37 nM to 30 μM in an 11-point curve and a final DMSO concentration of 0.3%. Each curve occurred in triplicate in each plate along with vehicle-matched controls. CRCs were generated using a Labcyte Echo 555 employed with Labcyte Dose Response Software package. Calcium flux was measured using the Functional Drug Screening System 6000 (FDSS 6000, Hamamatsu, Japan); compound alone was added at 3 seconds to detect any agonist activity followed by a EC_{20} of glutamate at 143 seconds and finally a EC_{80} glutamate at 240 seconds. A glutamate concentration (60 μM) resulting in a maximal response was also added in the third addition to wells not receiving compound or previous glutamate additions. The resulting EC_{max} response was used to normalize test responses during data analysis. FDSS data were analyzed using a Microsoft Excel analysis template using Excel formulas for data reduction and IDBS XLfit (Guildford, UK) for curve fitting. Each point was normalized to the initial value for that well (static ratio). For each window (agonist, potentiator, antagonist), the peak static ratio response was determined and corrected by subtraction of the minimum response at the beginning of the data collection. Each corrected response was then expressed as a percent of the average baseline corrected static ratio of the EC_{max}. For the agonist, potentiator, and antagonist windows, each corresponding $\%EC_{max}$ response was plotted versus the log of the molar concentration of test compound. The data were fit to a 4 parameter logistic equation to determine the minimum response, maximum response (% response achieved relative to the maximal response obtained with glutamate, % Glu_{max}), the log concentration giving the half-maximal response (log EC_{50}), and the slope factor of the curve.

DMD Fast Forward. Published on July 2, 2013 as DOI: 10.1124/dmd.113.052084
This article has not been copyedited and formatted. The final version may differ from this version.

$mGlu_1$ Selectivity Screening

HEK293A cells stably expressing rat $mGlu_1$ were plated in black-walled, clear-bottomed, poly-D-lysine coated 384-well plates (Greiner Bio-One, Monroe, NC) in assay medium at a density of 20,000 cells/well 24 hours prior to the assay. Assays were performed at the Vanderbilt University High-Throughput Screening Center as described previously (Rodriguez et al., 2010; Hammond et al., 2010). Calcium flux was measured using the FDSS 6000; vehicle or a fixed concentration of test compound (10 μM) was added followed by a concentration response curve to glutamate 2.5 minutes later. The change in relative fluorescence over basal was calculated before normalization to the maximal response to glutamate.

Group II and Group III mGlu Selectivity Screening

Test compound activity at the rat group II and III mGlus was assessed using thallium flux through GIRK channels as previously described in detail (Niswender et al., 2008; Hammond et al., 2010). Briefly, HEK293A-GIRK cells expressing mGlu subtypes (2, 3, 4, 6, 7 or 8) were plated into 384-well, black-walled, clear-bottom poly-D-lysine coated plates at a density of 15,000 cells/well in assay medium the day prior to the assay. On the day of the assay, the medium was aspirated and replaced with assay buffer (Hank's Balanced Salt Solution, 20 mM HEPES, pH 7.4) supplemented with 0.16 μM Fluozin2-AM (Invitrogen, Carlsbad, CA). For these assays, vehicle or fixed concentration of test compound (10 μM) was added followed by a concentration response curve to glutamate (or L-AP4 in the case of $mGlu_7$) diluted in thallium buffer (125 mM $NaHCO_3$, 1 mM $MgSO_4$, 1.8 mM $CaSO_4$, 5 mM glucose, 12 mM thallium sulfate, 10 mM HEPES), and fluorescence was measured using a FDSS 6000. Data were

DMD Fast Forward. Published on July 2, 2013 as DOI: 10.1124/dmd.113.052084
This article has not been copyedited and formatted. The final version may differ from this version.

analyzed as described previously (Niswender et al., 2008). The presence of activity at each receptor was determined by comparing the fold shift imparted by the compound (EC_{50} of glutamate under control conditions divided by EC_{50} in the presence of compound) as well as the effect on the maximum response of glutamate. A compound was determined to be a PAM if it resulted in a fold shift of 2.0 or greater, a NAM if it decreased the maximum response from 100% to 75% or less, and an antagonist if it resulted in a fold shift of 0.5 or less and the maximum response remained above 75%.

Ancillary Pharmacology Screening

VU0403602 was sent to Ricerca Biosciences (Painesville, OH) for testing in their LeadProfiling Screen, a panel of ancillary pharmacology binding assays measuring % displacement of an orthosteric radioligand at 66 distinct molecular targets. Two independent determinations were made using 10 μM test compound concentration. Significant activity was defined as >50% inhibition of binding at any target. Additionally, a functional 5-HT_{2B} assay was performed using rat stomach fundus ($N = 2$) and a 30 μM test compound concentration.

Radioligand Binding Assays

The allosteric antagonist MPEP analog [^{3}H]methoxyPEPy (Cosford et al., 2003) was used to evaluate the interaction of the test compounds with the allosteric MPEP site on $mGlu_5$. Membranes were prepared from HEK293A cells stably expressing rat $mGlu_5$. Compounds were diluted into assay buffer (50 mM Tris and 0.9% NaCl, pH 7.4) to a 2x stock, and 125 μL of test compound was added to each well of a 96-well assay plate. 100 μL aliquots of membranes diluted in assay buffer (50 μg/well) were added to each well. Twenty-five microliters of

DMD Fast Forward. Published on July 2, 2013 as DOI: 10.1124/dmd.113.052084
This article has not been copyedited and formatted. The final version may differ from this version.

[^{3}H]methoxyPEPy (5 nM final concentration in assay buffer) were added, and the reaction was incubated at room temperature for 60 min with shaking. After the incubation period, the membrane-bound ligand was separated from free ligand by filtration through glass fiber 96-well filter plates (Unifilter-96, GF/B; PerkinElmer Life and Analytical Sciences, Boston, MA). The contents of each well were transferred simultaneously to the filter plate and washed three times with assay buffer (Brandel cell harvester; Brandel Inc., Gaithersburg, MD). Forty microliters of scintillation fluid was added to each well, and the membrane-bound radioactivity was determined by scintillation counting (TopCount; PerkinElmer Life and Analytical Sciences). Nonspecific binding was estimated using 10 μM MPEP.

Animal Usage

All animal studies and experiments were conducted in accordance with the National Institutes of Health's *Guide for the Care and Use of Laboratory Animals* and were approved by the *Institutional Animal Care and Use Committee*. Animals were housed under a 12-hour light/dark cycle with access to food and water (*ad libitum*).

Electrophysiology

Extracellular field potential recordings. LTD experiments: 4-6 week old male Sprague–Dawley (SD) rats (Charles River, Wilmington, MA) were sacrificed and the brains quickly removed and submerged into ice-cold cutting solution (in mM: 110 sucrose, 60 NaCl, 3 KCl, 1.25 NaH_2PO_4, 28 $NaHCO_3$, 5 D-glucose, 0.6 (+)-sodium-L-ascorbate, 0.5 $CaCl_2$, 7 $MgCl_2$) continuously bubbled with 95% O_2/5% CO_2. 400 μm transverse brain slices were made using a vibratome (Leica VT100S; Leica Microsystems, Nussloch, Germany). Individual hippocampi were micro

dissected from the slice and transferred to a room temperature mixture containing equal volumes of cutting solution and artificial cerebrospinal fluid (ACSF; in mM: 125 NaCl, 2.5 KCl, 1.25 NaH_2PO_4, 25 $NaHCO_3$, 25 glucose, 2 $CaCl_2$, 1 $MgCl_2$) and allowed to equilibrate for 30 minutes. The hippocampi were then transferred to ACSF continuously bubbled with 95% O_2/5% CO_2 for a minimum of an additional hour. For recordings, slices were transferred to a submersion recording chamber and allowed to equilibrate for 5-10 minutes at 30-32°C with a flow rate of 2 mL/min. Schaffer collaterals were stimulated by placing a bipolar-stimulating electrode in the stratum radiatum near the CA3-CA1 border. Recording electrodes were pulled with a Flaming/Brown micropipette puller (Sutter Instruments, CA), filled with ACSF, and placed in the stratum radiatum of area CA1. Field potential recordings were acquired using a MultiClamp 700B amplifier (Molecular Devices, Sunnyvale, CA) and pClamp 10 software (Molecular Devices). Input–output curves were generated to determine the stimulus intensity that produced 50–60% of the maximum field excitatory postsynaptic potential (fEPSP) slope before each experiment, which was then used as the baseline stimulation. Test compounds were diluted to the appropriate concentrations in DMSO (0.1% final) in ACSF and applied to the bath for 10 minutes using a perfusion system. Chemically induced mGlu long-term depression (LTD) was initiated by the application of DHPG in ACSF (75 μM) for 10 minutes. Sampled data was analyzed offline using Clampfit 10. The slopes from three sequential fEPSPs were averaged. All fEPSP slopes were normalized to the average slope calculated during the predrug period (percent of baseline). Data were analyzed using GraphPad Prism.

Epileptiform experiments. Male SD rats (24-30 day old, Charles River) were sacrificed and the brains quickly removed and submerged into ice-cold cutting solution (same as above) continuously bubbled with 95% O_2/5% CO_2. 400 μm transverse slices were made as described

DMD Fast Forward. Published on July 2, 2013 as DOI: 10.1124/dmd.113.052084
This article has not been copyedited and formatted. The final version may differ from this version.

above. Individual hippocampi were transferred to artificial cerebrospinal fluid (ACSF; in mM: 124 NaCl, 5 KCl, 1.25 NaH_2PO_4, 26 $NaHCO_3$, 10 glucose, 2 $CaCl_2$, 1.2 $MgCl_2$), maintained at room temperature, and allowed to equilibrate for a minimum of 1 hour. For recordings slices were transferred to a submersion recording chamber and allowed to equilibrate for 5-10 minutes at 30-32°C with a flow rate of 2 mL/min. Recording electrodes were pulled with a Flaming/Brown micropipette puller (Sutter Instruments, CA), filled with ACSF, and placed in the cell body layer of CA3. Field potential recordings (spontaneous events) were acquired using a MultiClamp 700B amplifier (Molecular Devices, Sunnyvale, CA) and pClamp10 software (Molecular Devices). Compounds of interest were diluted to the appropriate concentrations in DMSO (0.1% final) in ACSF and applied to the bath for 10 minutes using a perfusion system. DHPG was used as a positive control (50 μM). Sampled data was analyzed offline using MiniAnalysis (Synaptosoft Inc., Fort Lee, NJ) to determine the amplitude and inter-event interval of the spontaneous events and normalized to the predrug period.

Plasma Protein Binding and Nonspecific Binding in Brain Homogenate

The extent of plasma protein binding and nonspecific binding of test compounds was determined *in vitro* in male (SD) rat plasma and brain homogenate via rapid equilibrium dialysis (RED; ThermoFisher Scientific, Rochester, NY). A 96 well plate containing plasma and an individual test article (5 μM) was vortex mixed. A portion (200 μL) of the mixture was transferred to the cis chamber of the RED insert and dialyzed against phosphate buffer (350 μL, 25 mM, pH 7.4) in the trans chamber and incubated (37°C) with shaking (4 hr). Following the incubation, an aliquot from each chamber was diluted (1:1; v/v) with either plasma or buffer from the cis or trans chamber, respectively, and transferred to a new 96 well plate. Protein precipitation of the

DMD Fast Forward. Published on July 2, 2013 as DOI: 10.1124/dmd.113.052084
This article has not been copyedited and formatted. The final version may differ from this version.

matrices was executed by the addition of ice-cold acetonitrile containing carbamazepine (50 nM) as an internal standard for LC-MS/MS analysis. The plate was centrifuged (3000 RCF, 10 min) and the supernatants transferred to a new 96 well plate where they were diluted in H_2O (1:1; v/v). The plate was then sealed for LC/MS/MS analysis.

Hepatic Microsome Stability Assessment of VU0403602

The metabolic stability of VU0403602 was investigated in male SD rat hepatic microsomes using substrate depletion methodology (% parent compound remaining). In 96-well plate a potassium phosphate-buffered (0.1 M, pH 7.4) solution of VU0403602 (1 μM), microsomes (0.5 mg/mL), + NADPH (1 mM), + $MgCl_2$ (3 mM) was incubated at 37 °C under ambient oxygenation; reactions were initiated by the addition of NADPH. At designated times (t = 0, 3, 7, 15, 25, and 45 min) an aliquot of the incubation mixture was removed and precipitated by the addition of two volumes of ice-cold acetonitrile containing carbamazepine as an internal standard (50 ng/mL). The plates were centrifuged at 3000 RCF (4 °C) for 10 min. The resulting supernatants were diluted 1:1 (supernatant: water) into a new 96-well plates in preparation for LC/MS/MS analysis. The compound was assayed in triplicate within the same 96-well plate. The substrate depletion methodology previously described was used to estimate the *in vitro* intrinsic clearance (CL_{int}; mL/min/kg) of VU0403602 in rat liver microsomes(Obach and Reed-Hagen, 2002).

Hepatic Biotransformation of VU0403602

The *in vitro* metabolism of VU0403602 was investigated in hepatic S9 fractions from SD rats (male, pooled; BD Biosciences, San Jose, CA). A potassium phosphate-buffered solution (0.1

DMD Fast Forward. Published on July 2, 2013 as DOI: 10.1124/dmd.113.052084
This article has not been copyedited and formatted. The final version may differ from this version.

M, pH 7.4) of test compound (25 μM) and hepatic S9 fractions (5 mg/mL) was incubated (37°C) in borosilicate glass tubes under ambient oxygenation for 1 hour with select reactions being fortified with NADPH (2 mM), UDGPA (2 mM), and/or PAPS (2 mM). Protein was precipitated by the addition of two volumes of acetonitrile with subsequent centrifugation (3000 RCF, 10 min). The supernatant was dried under a stream of nitrogen gas and reconstituted in 85:15 (v/v) ammonium formate (10 mM, pH 4.1, aqueous):acetonitrile in preparation for LC/MS/MS analysis. In an identical manner, and where indicated, the metabolism of VU0403602 was investigated in SD rat intestinal S9 fractions (4 mg/mL, pooled male SD rats, BD Biosciences, San Jose, CA).

Pharmacokinetic Studies in Rats Following Intravenous Administration

Male SD rats (250-300 g) were purchased from Harlan Laboratories (Indianapolis, IN). Catheters were surgically implanted in the carotid artery and jugular vein. The cannulated animals were acclimated to their environment for approximately one week before dosing. Parenteral administration of test compounds to rats was achieved via a jugular vein catheter at a dose of 1 or 3 mg/kg and a dose volume of 1 mL/kg (10% EtOH/50% PEG 400/40% saline) or 3 mL/kg (10% EtOH/90% PEG 400) for metabolite **M1** and parent VU0403602, respectively. Blood collections via the carotid artery were performed at 2, 7, 15, and 30 minutes and 1, 2, 4, 7, and 24 hours post administration. Samples were collected into chilled, EDTA-fortified tubes, centrifuged for 10 minutes (3000 RCF, 4 °C), and the resulting plasma stored at -80ºC until analysis. Pharmacokinetic parameters were obtained from noncompartmental analysis (NCA, WinNonLin, v5.3, Pharsight Corp., Mountain View, CA) of individual animal concentration-time profiles following the parenteral administration of a test compound.

DMD Fast Forward. Published on July 2, 2013 as DOI: 10.1124/dmd.113.052084
This article has not been copyedited and formatted. The final version may differ from this version.

Determination of Systemic and CNS Exposure of VU0403602

Male SD rats (250-300 g) were purchased from Harlan Laboratories (Indianapolis, IN) and acclimated to their surroundings for approximately one week before dosing. Intraperitoneal (IP) administration of test compounds to rats was performed at various doses (3 to 30 mg/kg). When warranted, rats received pre-treatment with ABT (PO, 50 mg/kg) or co-administration of test article and MPEP (IP, 5 or 10 mg/kg)(Balani, 2002). Plasma and whole brains were collected at varied time points using non-serial sampling methods from multiple animals. Plasma samples were collected into chilled, EDTA-fortified tubes, centrifuged for 10 minutes (3000 rcf, 4 °C), and the resulting plasma stored at -80ºC until analysis. Brain samples were rinsed with cold phosphate-buffered saline, snap frozen (dry ice) and stored at -80 ºC until LC/MS/MS analysis. Plasma and brain time-concentration area-under-the-curves (AUCs) were calculated by the trapezoidal method employing Prism software (GraphPad, La Jolla, CA).

Behavioral Manifestations of Seizure Activity

To study $mGlu_5$ PAM-induced behavioral manifestation of seizure activity, rats received various doses (IP; 30 mg/kg) of the test compound +/- the $mGlu_5$ antagonist MPEP (5 and 10 mg/kg). Compounds were formulated in 10% Tween 80 and administered at a volume of 3 mL/kg. Animals were monitored continuously for 2 hr. After this procedure, rats were euthanized and brains removed and processed for compound exposure levels. Rats were scored for behavioral manifestations of seizure activity in periods of 5 min, once every 5 min for the first 15 min, then once every 15 min up to 1 hr, and every 30 minutes up to 2 hr. Compound-induced behavioral manifestations of seizures were scored using a five grade modified Racine scoring system (Rook

DMD Fast Forward. Published on July 2, 2013 as DOI: 10.1124/dmd.113.052084
This article has not been copyedited and formatted. The final version may differ from this version.

2012). A score of 0 represents no behavioral alteration; score 1, immobility, mouth and facial movements, facial clonus; score 2, head nodding, forelimb and/or tail extension, rigid posture; score 3, forelimb clonus, repetitive movements; score 4, rearing, forelimb clonus with rearing, rearing and falling; and score 5, continuous rearing and falling, jumping, severe tonic-clonic seizures.

Reversal of Amphetamine-Induced Hyperlocomotion

Studies were conducted using male SD rats purchased from Harlan Laboratories (Indianapolis, IN) weighing 275 to 300 g. Dose groups consisted of 5 to 12 rats per group. VU0403602 was dissolved in 10% Tween 80 and double-deionized water and the pH was adjusted to approximately 7.0 using 1 N NaOH. VU0403602 was administered IP at a dose of 3, 10, or 30 mg/kg in a 3 mL/kg volume. Studies were performed as previously described (Noetzel et. al., 2011). Briefly, rats were placed in the open-field chambers and allowed to habituate for 30 minutes followed by pretreatment (IP) with vehicle or test compound. After an additional 30 minutes, rats received a saline vehicle or 1 mg/kg amphetamine via subcutaneous (SC) injection. Locomotor activity was measured for an additional 60 minutes. Ambulation or locomotor activity was measured as the number of total photobeam breaks per 5-minute interval using Motor Monitor System software (KinderScientific). Main effects of test compound treatment on the amphetamine-induced locomotor activity area under the time course curve were evaluated using one-way analysis of variance. Comparisons of treatment group effects relative to the vehicle + amphetamine group were completed across the time interval from t = 60 to 120 min using Dunnett's post hoc tests with a p value of < 0.05 considered significant.

DMD Fast Forward. Published on July 2, 2013 as DOI: 10.1124/dmd.113.052084
This article has not been copyedited and formatted. The final version may differ from this version.

Liquid Chromatography-UV-Mass Spectrometry Analysis of VU0403602 and Corresponding Metabolites

Plasma and brain tissue samples originating from *in vivo* studies were analyzed with electrospray ionization by an AB Sciex Q-TRAP 5500 (Foster City, CA) that was coupled to a Shimadzu LC-20AD pumps (Columbia, MD) and a Leap Technologies CTC PAL auto-sampler (Carrboro, NC). Analytes were separated by gradient elution using a C18 column (3 x 50 mm, 3 μm; Fortis Technologies Ltd, Cheshire, UK) that was thermostated at 40 °C. HPLC mobile phase A was 0.1% formic acid in water (pH unadjusted), mobile phase B was 0.1% formic acid in acetonitrile (pH unadjusted). A 30% B gradient was held for 0.2 min and was linearly increased to 90% B over 0.8 min, with an isocratic hold for 0.6 min, prior to transitioning to 30% B over 0.1 min. The column was re-equilibrated (1 min) prior to the next sample injection. The total run time was 2.5 min and the HPLC flow rate was 0.5 mL/min. The source temperature was set at 500 °C and mass spectral analyses were performed using multiple reaction monitoring (MRM) of transitions specific for the test articles and metabolites, and utilizing a Turbo-Ionspray® source in positive ionization mode (5.0 kV spray voltage). All data were analyzed using AB Sciex Analyst 1.5.1 software. The lower limits of quantitation for VU0403602, VU0453103 (**M1**), and VU0451326 (**M2**), were determined at 1 ng/mL in plasma and 0.5 ng/g in brain homogenate.

Samples from *in vitro* DMPK assays (CL_{int}, plasma protein and brain homogenate binding), were analyzed on a TSQ Quantum Ultra (Thermo Fisher Scientific, Waltham, MA) utilizing electrospray ionization (ESI). The mass spectrometer was coupled to an Accella HPLC pump system (Thermo Fisher Scientific, Waltham, MA) and a CTC PAL autosampler. Analytes were separated by gradient elution employing two Acquity BEH C18 columns (2.1 x 50 mm, 1.7 μ; Waters Corp., Milford, MA) that were heated at 50 °C. HPLC mobile phase A was a

DMD Fast Forward. Published on July 2, 2013 as DOI: 10.1124/dmd.113.052084
This article has not been copyedited and formatted. The final version may differ from this version.

95:5:0.1 mixture of water:acetonitrile:formic acid, respectively; mobile phase B was a 95:5:0.1 mixture of acetonitrile:water:formic acid, respectively. The following was the gradient program that was employed in these separations: pump 1 ran the gradient: 95:5 (A:B) at 800 µL/min hold 0 to 0.5 min, linear ramp to 5:95 (A:B) 0.5 to 1.0min, 5:95 (A:B) hold 1.0 to 1.9 min, return to 95:5 (A:B) at 1.9 min. While pump 1 ran the gradient method, pump 2 equilibrated the previously used column under isocratic conditions (95:5; A:B). The total run time was 2.0 minutes. All compounds were optimized and analyzed using QuickQuan (Thermo Fisher Scientific, Waltham, MA) software.

Samples from *in vitro* metabolism experiments and authentic standards of test compound/metabolites were analyzed on an Agilent 1100 HPLC system employing a Supelco Discovery C18 column (2.1 x 150 mm, 5 µm; Sigma-Aldrich Chemical Company, St. Louis, MO). Solvent A was 10 mM (pH 4.1) ammonium formate and solvent B was acetonitrile. The initial mobile phase was 15% and by linear gradient transitioned to 80% over 20 min. The flow rate was 0.400 mL/min. The HPLC eluent was first introduced into an Agilent 1100 DAD (single wave length selected, 254 nM) followed by electrospray ionization introduction into a Finnigan LCQ™ Deca XP^{PLUS} ion trap mass spectrometer (Thermo Fisher Scientific., Waltham, MA) operated in either the positive or negative ionization mode. Ionization was assisted with sheath and auxiliary gas (ultrapure nitrogen) set at 60 and 40 psi, respectively. The electrospray voltage was set at 5 kV with the heated ion transfer capillary set at 300°C and 30 V. Relative collision energies of 25-35% were used when the ion trap mass spectrometer was operated in the MS/MS or MS^n mode.

Results:

DMD Fast Forward. Published on July 2, 2013 as DOI: 10.1124/dmd.113.052084
This article has not been copyedited and formatted. The final version may differ from this version.

VU0403602 Displays a Mixed $mGlu_5$ Agonist-PAM Pharmacology Profile *In Vitro*. We previously reported a series of small molecule selective $mGlu_5$ PAMs that were developed based on a biaryl acetylene scaffold; a number of highly potent compounds were identified that display *in vivo* activity in rodent behavioral models of antipsychotic efficacy(Williams et al., 2011; Rook et al., 2012). We recently identified a cyclobutyl picolinamide analog VU0403602 that displayed potent $mGlu_5$ agonist (31.1 nM, 49% Glu_{max}) and PAM (4 nM, 100% Glu_{max}) activity *in vitro* (Figure 2), inducing a progressive concentration-dependent left-shift (9-fold maximal shift at 1 μM, data not shown) of the glutamate concentration-response curve (CRC) in a functional calcium mobilization assay in $mGlu_5$-expressing HEK293A cells(Gregory et al., 2013). Importantly, VU0403602 is absent of activity at $mGlu_1$ (Ca^{2+} assay), group II (GIRK thallium flux assay), and group III receptors (GIRK thallium flux assay), indicating the compound is a subtype-selective $mGlu_5$ ligand (Supplemental Figure 1). VU0403602 displayed minimal off-target ancillary pharmacology, as radioligand binding displacement of a broad panel (> 65) of GPCRs, ion channels, transporters, and other targets (N = 2, 10 μM test compound) indicated significant activity (>50%) for only three targets: human norepinephrine transporter (NET, 66% inhibition), human dopamine transporter (DAT, 67% inhibition), and a human serotonin receptor (5-HT_{2B}, 92% inhibition). Subsequent 5-HT_{2B} functional assays with VU0403602 (30 μM) in rat stomach fundus tissue revealed no significant activity (data not shown).

Competition binding experiments using the MPEP site radioligand [^{3}H]-mPEPy to label membranes from rat mGlu5-expressing HEK cells revealed a fully competitive interaction by VU0403602, similar to that of the unlabeled MPEP control (Supplemental Figure 2). In additional cell-based functional experiments using $mGlu_5$-expressing cells, concentration-

DMD Fast Forward. Published on July 2, 2013 as DOI: 10.1124/dmd.113.052084
This article has not been copyedited and formatted. The final version may differ from this version.

response curves (CRCs) of VU0403602 in the presence of multiple fixed concentrations of the noncompetitive $mGlu_5$ antagonist, 5PMEP (occupies the MPEP allosteric site), exhibited parallel right-shifts, with a corresponding Schild regression analysis indicating a competitive mode of interaction (slope = 1.06)). These data support a fully competitive interaction of VU0403602 at the prototypical MPEP binding site of $mGlu_5$.

***In Vivo* Administration of VU0403602 Induces Adverse Events in Rats.** Although VU0403602 produced a dose-dependent (3, 10, 30, mg/kg, IP; ED_{50}, 21 mg/kg) efficacy in the reduction of hyperlocomotion in SD rats (Supplemental Figure 3) receiving amphetamine (1 mg/kg, SC), the systemic administration of this $mGlu_5$ PAM also induced pronounced adverse events (AEs) marked by the onset of seizures, forelimb asymmetry, tremor, and facial bleeding, the severity of which were recorded using the Racine assessment method (Rook 2012). The onset of VU0403602-mediated AEs was similar to those observed in SD rats that received a single administration (IP) of the Ago-PAM VU0424465 (Agonist EC_{50}: 171 nM, 65% Glu_{max}, PAM EC_{50}: 2 nM, 88% Glu_{max}; Rook 2012). When rats received a single IP dose (30 mg/kg) of VU0403602 in the absence of amphetamine, subsequent observations revealed a time-dependent manifestation of the aforementioned behavioral effects (Figure 3). To determine whether the AEs observed in rats were $mGlu_5$ target-mediated, we administered (IP) VU0403602 (30 mg/kg) with the $mGlu_5$ allosteric antagonist, MPEP (5 and 10 mg/kg), and monitored the behavioral effects for four hours post-treatment. The lower dose (5 mg/kg) of MPEP reduced the severity of the VU0403602-induced behavioral AEs by approximately 50%, whereas rats receiving the 10 mg/kg dose of MPEP were completely devoid of the behavioral manifestations (Figure 3). These data implicate a role for $mGlu_5$ in the mechanism underlying the AEs resulting from the

administration of VU0403602. Interestingly, pretreatment of rats with the pan cytochrome P450 inactivator, 1-aminobenzotriazole (ABT; 50 mg/kg, IP), completely mitigated the onset of the behavioral AEs resulting from the systemic administration of VU0403602, indicating that one or more metabolites of this PAM may be contributing to the $mGlu_5$–mediated toxicity observed *in vivo* (Figure 3)(Balani, 2002).

The *In Vitro* and *In Vivo* Disposition of VU0403602 in Sprague-Dawley Rats Reveals Hepatic Metabolism as the Mechanism of Clearance. Following the initial rat behavioral findings, the DMPK profile of VU0403602 was determined using conventional *in vitro* subcellular fraction metabolism and *in vivo* dosing paradigms to define the biotransformation pathways for VU0403602 and the contribution(s) of metabolites towards precipitating AEs in rat(Balani et al., 2005). The intrinsic clearance (CL_{int}) of VU0403602 was assessed in rat hepatic microsomes and subsequently used to predict the extent of hepatic clearance (CL_{hep}) *in vivo*. The CL_{int} and CL_{hep} values (271 mL/min/kg and 55.6 mL/min/kg, respectively) for VU0403602 correlated well with the total body plasma clearance value (CL_p: 36.2 mL/min/kg) observed in rats following parenteral administration (3 mg/kg) (Supplemental Figure 4), indicating that hepatic metabolism was likely the predominant mechanism of clearance for VU0403602. Consistent with this assessment, we detected negligible amounts of unchanged VU0403602 excreted in the urine. The volume of distribution estimated at steady-state of VU0403602 (V_{ss}, 6.73 L/kg) exceeded that of the total body water in rats, and coupled with its moderate CL_p *in vivo*, resulted in a mean residence time (MRT) of approximately 3 hours (Supplemental Figure 4). *In vitro* rapid equilibrium dialysis (RED) indicated the plasma protein binding of VU0403602 to be extensive in rat plasma, producing a corresponding fraction unbound (F_u) of

DMD Fast Forward. Published on July 2, 2013 as DOI: 10.1124/dmd.113.052084
This article has not been copyedited and formatted. The final version may differ from this version.

< 0.01; RED data also indicated extensive nonspecific binding of VU0403602 (F_u < 0.01) in rat brain homogenate.

***In Vitro* Biotransformation of VU0403602 Results in the Formation of Two Principal Metabolites.** Liquid chromatographic, tandem mass spectrometry analysis (LC/MS/MS) was used to characterize the metabolites of VU0403602 produced *in vitro* from rat S9 fractions (intestinal, hepatic, brain), potentially representing metabolite-ligands of $mGlu_5$ that could contribute to the AEs observed in rats. Data from these experiments revealed two principal biotransformation pathways for VU0403602 (Scheme 1), NADPH-dependent oxidation of the cyclobutyl moiety of VU0403602 to the hydroxylated metabolite, **M1**, and the NADPH-independent amide hydrolysis of VU0403602 to the carboxylic acid metabolite, **M2**. Metabolite **M1** was observed at approximately 16.1 minutes as the $[M+H]^+$ at *m/z* 311 (Figure 4). The primary fragmentation observed (100% relative) was the gas phase loss of water (-18 Da; $-H_2O$) to produce the ion at *m/z* 293, representing a 16 Da increase over the water loss fragment observed in the MS/MS of VU0403602 (*m/z* 277). A secondary fragmentation from the ion at *m/z* 293 was also observed in the MS/MS of **M1** (*m/z* 275). Another fragmentation observed for **M1** was the gas phase, water-assisted fragmentation of the amide bond that resulted in the formation of an ion at *m/z* 242 (20% relative). The water-assisted amide fragmentation was also observed in the MS/MS of VU0403602, producing a fragment ion at *m/z* 242 in addition to the loss of the cyclobutyl moiety producing an $[M+2H]^+$ at *m/z* 241. The proposed carboxylic acid metabolite **M2**, observed at 15.7 minutes ($[M+H]^+$ at *m/z* 242), resulted in the gas phase decarboxylation of **M2**, producing a fragment ion at *m/z* 196.

DMD Fast Forward. Published on July 2, 2013 as DOI: 10.1124/dmd.113.052084
This article has not been copyedited and formatted. The final version may differ from this version.

To determine the relative stereochemistry of oxidation of the cyclobutyl moiety of VU0403602 to the hydroxylated metabolite, **M1**, we synthetically prepared authentic *cis* and *trans* hydroxylated compounds from the cis/trans 3-hydroxy-1-amino-cyclobutane and a requisite amide coupling; chiral SFC was employed to separate the *cis* and *trans* standards (Supplemental Schemes 1-3). The *cis* (VU0453102) and *trans* (VU0453103) structures were confirmed based upon both 1D NMR studies (Supplemental Figures 5-8), including the examination of Nuclear Overhauser Effects (NOE) between the methine protons within the cyclobutane ring system (Supplemental Figure 9). Subsequent LC/MS/MS analysis confirmed the stereochemistry of **M1** as that of the *trans* compound (a.k.a., VU0453103) based on the corresponding LC retention time and MS/MS fragmentation pattern. The structure proposed for **M2** was also confirmed via LC/MS/MS comparison with its authentic standard (VU0451326).

The Hydroxylated Metabolite (M1) is a Metabolite-Ligand of $mGlu_5$ Displaying Agonist and PAM Activity. A pharmacological characterization of **M1** on the $mGlu_5$ receptor was obtained through the use of functional calcium mobilization assays measuring agonist, PAM, and antagonist responses at $mGlu_5$ in recombinant HEK293A cells. *In vitro* analysis revealed **M1** to be a robust ago-PAM, possessing agonist and PAM EC_{50} values of 400 nM (78% Glu_{max}) and 16.9 nM (94% Glu_{max}), respectively (Figure 5). Related glutamate CRC experiments demonstrated that **M1** (10 μM) induced a maximal left-shift of 8.2-fold, similar to that of 9-fold for the parent PAM, VU0403602 (1 μM, data not shown). However, unlike the partial $mGlu_5$ agonist activity of the parent VU0403602 (49.4% Glu_{max}), the hydroxylated metabolite **M1** displayed a near full agonist activity (94% Glu_{max}). By contrast, the carboxylic acid metabolite

DMD Fast Forward. Published on July 2, 2013 as DOI: 10.1124/dmd.113.052084
This article has not been copyedited and formatted. The final version may differ from this version.

(**M2**) displayed no activity at $mGlu_5$ up to the limit of solubility (agonism, PAM, antagonism EC_{50} values > 30 μM, data not shown).

The *In Vivo* Metabolism of VU0403602 Resulted in the Formation and Distribution to the CNS of the Active Metabolite-ligand, M1. Based on the abundant formation *in vitro* and the potent $mGlu_5$ pharmacological activity observed for **M1**, we suspected that the systemic formation and CNS exposure of this hydroxylated metabolite *in vivo* may contribute to the adverse events observed in rats. Moreover, a role of **M1** in eliciting the AEs in rats would be consistent with the ABT results, where the absence of AEs was noted in rats that had received the single pretreatment with the P450 inactivator, ABT. Therefore, we administered VU0403602 to rats (IP, 30 mg/kg; $N = 2$) that were treated with either ABT (P.O., 50 mg/kg) or vehicle (0.5% methylcellulose in water) followed by brain and blood collections (1.5 hr post dose) in order to determine the concentrations of VU0403602 and its metabolites (**M1** and **M2**) in the plasma and CNS (Table 1). The separation of plasma and brain homogenates was first demonstrated with a protracted LC/MS/MS gradient in order to qualitatively profile the range of metabolites observed *in vivo*; results from this LC/MS/MS analysis indicated that VU0403602, **M1**, and **M2** were the principal components observed *in vivo*, with a negligible component observed representing the *cis*-isomer of **M1**. Hence, the remaining quantitative bioanalysis of plasma and brain homogenate samples was executed with a standard high throughput LC/MS/MS gradient as described above without the resolution of the *cis* and *trans*-hydroxylated metabolites. In the absence of ABT, VU0403602 reached an average maximal concentration (C_{max}) of 3.2 μM (5 nM unbound) with a corresponding time to reach C_{max} (T_{max}) of 0.25 hr in plasma; the C_{max} observed in brain was 11.5 μM (6 nM, unbound) with an average T_{max} of 0.88 hr (Table 1). In

DMD Fast Forward. Published on July 2, 2013 as DOI: 10.1124/dmd.113.052084
This article has not been copyedited and formatted. The final version may differ from this version.

plasma, **M1** reached an average total C_{max} of 64 nM (4 nM unbound) with an average T_{max} of 0.25 hr (Table 1). The brain penetration observed for **M1** was substantial, reaching an approximate 9:1 distribution relative to the systemic plasma compartment. **M1** reached an average brain C_{max} of 400 nM (4 nM, unbound) and a corresponding T_{max} of 1.5 hr (Table 1). Due the extensive plasma protein- and nonspecific-binding of VU0403602 (F_u << 0.01) and **M1** (F_u, 0.01) observed *in vitro*, the framing of the relevant concentrations observed between the two tissue compartments (i.e., systemic circulation and the CNS) may be most appropriate when considering the total concentrations achieved. Moreover, this framing of concentrations may also be best applied to the pharmacological activity elicited by VU0403602 and **M1** *in vivo*. However, regardless of consideration of total and/or unbound levels achieved, the results obtained from *in vivo* analysis are consistent with that generated from the *in vitro* metabolism experiments; rats that had received the P450 inactivator ABT, produced an approximate 11-fold lower C_{max} of the hydroxylated metabolite **M1** in plasma (13-fold lower C_{max}, brain) relative to the vehicle control (- ABT) treated rats (Table 1). Likewise, ABT pretreatment also reduced the area-under-the-curve ($AUC_{0\text{-}6h}$) of **M1** in plasma by approximately 17-fold in rats receiving a single administration (IP) of VU0403602, with a corresponding 8.4-fold reduction in the brain $AUC_{0\text{-}6}$ of **M1** (Table 1). Overall, the impact of ABT pretreatment on the metabolism of VU0403602 was profound, resulting in the substantial reduction of **M1** exposure *in vivo*, both in terms of maximal plasma and brain levels and systemic exposure. As expected for a nonP450-mediated biotransformation such as amide hydrolysis, ABT pretreatment had little to no effect on the C_{max} or $AUC_{0\text{-}6h}$ of the carboxylic acid metabolite, **M2**. Collectively, these data demonstrate the *in vivo* relevance of the $mGlu_5$ ago-PAM metabolite-ligand, **M1**, in the onset of adverse behavioral events observed in rats receiving IP administration of VU0403602.

DMD Fast Forward. Published on July 2, 2013 as DOI: 10.1124/dmd.113.052084
This article has not been copyedited and formatted. The final version may differ from this version.

***In Vitro* Rat Brain Slice Electrophysiology.**

VU0403602 and its hydroxylated metabolite M1 induce long-term depression in rat hippocampus. We and others have demonstrated the induction of long-term depression (LTD) at the Schaffer-collateral-CA1 (SC-CA1) synapse in the hippocampus as a result of $mGlu_5$ activation by orthosteric agonists as well as allosteric ago-PAMs. Importantly, we have demonstrated allosteric $mGlu_5$ modulators displaying exclusive PAM pharmacology are incapable of inducing LTD in the absence of an orthosteric ligand (e.g., DHPG). As previously discussed, the allosteric modulator VU0403602 displayed mixed ago-PAM pharmacology at $mGlu_5$ in recombinant cells expressing the rat receptor. To demonstrate the ago-PAM behavior of VU0403602 in a native system, we investigated alterations in electrophysiological responses in rat brain slices following *in vitro* exposure to VU0403602. Data generated from these experiments indicated that VU0403602 (10 μM) induced pronounced hippocampal LTD at the SC-CA1 synapse (Figure 6), with a prolonged depression of the field excitatory postsynaptic potential (fEPSP slope, 39.8 ± 5.9 % of baseline) well after the compound had been washed from the slice preparation (55 min post washout). Likewise, the hydroxylated metabolite **M1** (10 μM) also induced significant LTD at the SC-CA1 synapse (Figure 8) with a similar magnitude of depression of the fEPSP (slope 68.9 ± 4.9 % of baseline) and duration of action (55 min post washout). (Figure 6).

VU0403602 and metabolite M1 induce epileptiform activity in the rat hippocampal CA3 region in vitro. Having demonstrated that VU0403602 and its principal oxidative metabolite **M1** were capable of inducing alterations in LTD, additional experiments investigating whether these ago-PAMs are capable of inducing epileptiform activity in rat hippocampus, specifically in CA3

DMD Fast Forward. Published on July 2, 2013 as DOI: 10.1124/dmd.113.052084
This article has not been copyedited and formatted. The final version may differ from this version.

pyramidal neurons, were performed. Similar to the agonist DHPG, the hydroxylated metabolite **M1** (10 μM) and parent VU0403602 (10 μM) induced pronounced epileptiform activity as evidenced by decreases in the inter-event intervals of spontaneous field population spikes (48.1 ± 7.8 % and 48.8 ± 11 % of baseline, respectively) detected by extracellular field potential recordings in the pyramidal cell body layer of area CA3 in the hippocampal slices (Figure 7). Similar to the positive control DHPG (50 μM), neither VU0403602 nor **M1** significantly affected the amplitude of spontaneous events (Figure 7). Together, results from the rat hippocampal electrophysiology experiments indicate that the principal oxidative metabolite-ligand **M1** is capable of inducing LTD and epileptiform activity in native systems, a finding consistent with $mGlu_5$ activation and one that advances our understanding of the mechanism of AEs observed in rats receiving systemic administration of the parent compound, VU0403602.

Direct Administration of M1 Results in Behavioral AEs in Rats. The systemic administration of **M1** to rats was executed to determine whether this $mGlu_5$ metabolite-agonist was capable of inducing the pronounced AEs that we observed following the administration of the parent ligand VU0403602. Previously, following VU0403602 administration to rats (IP, 30 mg/kg), we observed a rapid T_{max} of both the parent ligand VU0403602 (T_{max}, 0.25 hr) and **M1** (T_{max}, 0.25 hr) as well a concurrent onset of behavioral AEs that marked this rodent neurotoxicity. Following direct administration of **M1** to rats (IP, 30 mg/kg) we observed a similar rapid onset of AEs (Figure 8). Moreover, the **M1**-mediated AEs were strikingly similar to those achieved by systemic administration of VU0403602 and the aforementioned ago-PAM, VU0422465, the occurrence of which were characterized by seizures, forelimb asymmetry, tremor, and facial bleeding. Considering the rapid formation of **M1** *in vivo*, its extensive distribution to the CNS,

DMD Fast Forward. Published on July 2, 2013 as DOI: 10.1124/dmd.113.052084
This article has not been copyedited and formatted. The final version may differ from this version.

and the consistency between the P450-mediated formation of **M1** and the subsequent mitigation of AEs following ABT pretreatment, we submit that this metabolite contributes to the *in vivo* toxicity observed in rats via an $mGlu_5$ receptor-mediated mechanism.

DMD Fast Forward. Published on July 2, 2013 as DOI: 10.1124/dmd.113.052084
This article has not been copyedited and formatted. The final version may differ from this version.

Discussion:

In an effort to advance new approaches in the treatment of the negative and cognitive symptoms common amongst schizophrenia patients, we have identified PAMs of $mGlu_5$ as potential novel therapeutics to rescue the NMDAR hypofunction believed to underpin this devastating neurological disorder(Olney et al., 1999; Tsai and Coyle, 2002; Williams et al., 2011; Rook et al., 2012). Herein, we have introduced an $mGlu_5$ PAM, VU0403602, residing within a biarylacetylene scaffold that, in addition to displaying robust potency and a corresponding 9-fold shift in the glutamate response, also displayed an intrinsic partial agonist profile *in vitro* (31.1 nM; 49% Glu_{max}). Such ago-PAMs have previously been shown to produce efficacy in preclinical models of psychosis, such as in the reversal of amphetamine-induced hyperlocomotion (AHL) rodent model(Noetzel et al., 2012; Rook et al., 2012). Indeed, following IP administration of VU0403602 to SD rats, VU0403602 produced a dose-dependent reversal of hyperlocomotion, with a minimally active dose of 3 mg/kg.

However, similar to previous reports from our laboratories regarding the systemic administration of ago-PAMs to rodents (e.g., VU0422465), we observed an adverse effect (AE) profile in rats following systemic administration of VU0403602 characterized by behavioral disturbances such as seizure activity(Noetzel et al., 2012; Rook et al., 2012). The onset of behavioral disturbances was dose and concentration-dependent, and the severity of the AEs increased with time as measured by Racine scoring methodology. Moreover, the neurotoxicity observed in rats was discovered to be target-mediated, as co-administration of VU0403602 with an allosteric antagonist of $mGlu_5$ (MPEP) effectively blocked the onset of AEs. Interestingly, an *in vitro* metabolism appraisal implicated oxidative metabolism as the primary biotransformation pathway for VU0403602, resulting in the formation of a principal hydroxylated metabolite **M1**

DMD Fast Forward. Published on July 2, 2013 as DOI: 10.1124/dmd.113.052084
This article has not been copyedited and formatted. The final version may differ from this version.

(+16 Da) in SD rat hepatic subcellular fractions (e.g., S9). Having demonstrated the P450-mediated mechanism of **M1** formation *in vitro*, we examined the extent of P450 metabolism *in vivo* and determined **M1** to be the principal oxidative metabolite detected in the circulation and central nervous system (i.e., brain tissue analysis) of rats receiving VU0403602(Kalvass and Maurer, 2002; Liu et al., 2008). Moreover, the distribution of **M1** to the CNS ($AUC_{0-\infty}$) was discovered to be approximately ~6:1 relative to the plasma of rats receiving VU0403602. Coupled with an unbound brain fraction (f_u) of 0.011 for **M1**, the CNS distribution of the primary oxidative metabolite (**M1**) far exceeded that of the parent modulator, VU0403602 ($AUC_{0-\infty}$ brain-to-plasma, ~2:1; brain f_u, <0.001).

Previously established structure-activity relationships (SAR) for allosteric modulation of $mGlu_5$ indicated a range of tolerance for oxidation (e.g., hydroxylation) of this scaffold with respect to resulting PAM activity of analogs, including switches in primary pharmacology to negative allosteric modulators (NAMs) and silent allosteric modulators (SAMs)(Sharma et al., 2009; Lindsley, 2011; Wood et al., 2011). Considering mono hydroxylation of organic molecules is a common outcome of P450–mediated metabolism, we hypothesized a role of drug metabolizing enzymes (DMEs) in the AEs observed *in vivo* following VU0403602 administration to rats. Importantly, rats that were pretreated with the pan P450 inactivator, ABT, failed to manifest the AEs previously demonstrated following VU0403602 exposure, implicating the role of an oxidative metabolite (e.g., **M1**) in the induction of *in vivo* neurotoxicity. Indeed, *in vitro* investigations revealed a pharmacological profile for **M1** characterized by a mixed ago-PAM profile in rat $mGlu_5$-expressing cells. Although the PAM efficacy of **M1** was similar to VU0403602 (8.2- and 9.0-fold left-shift in glutamate potency, respectively), we noted an agonist profile of higher efficacy for the metabolite (≈ 80% Glu_{max}) compared to that of VU0403602

DMD Fast Forward. Published on July 2, 2013 as DOI: 10.1124/dmd.113.052084
This article has not been copyedited and formatted. The final version may differ from this version.

(<50% Glu_{max}). Likewise, the ago-PAM character of **M1** was observed in the electrophysiological assessments, as exposure of rat hippocampal slices to the metabolite alone induced profound LTD at the SC-CA1 synapse, as well as epileptiform activity in area of CA3 of the hippocampus. The present findings are in agreement with previous data from our laboratory and other recent reports demonstrating that direct agonists and mixed ago-PAMs can over activate $mGlu_5$ and perturb normal neuronal activity in rats, which can include an induction of epileptiform activity in distinct hippocampal regions (e.g., CA3)(Lee et al., 2002; Wong et al., 2005; Rook et al., 2012). Although VU0403602 was able to induce LTD and epileptiform activity *in vitro*, its intrinsic partial agonism and overall lower efficacy *in vivo* appears insufficient to induce overt adverse effects on its own (i.e., in the presence of the P450 inactivator ABT) and at the concentrations achieved in the present studies. It is also possible that VU0403602 and **M1** may have differential effects in varied brain regions that are known to express $mGlu_5$. Ultimately, these findings serve to underscore the importance of avoiding allosteric agonist activity in the design of $mGlu_5$ modulators and thereby retaining dependency on activation of $mGlu_5$ by endogenous glutamate activity for the safe and efficacious modulation of $mGlu_5$.

Recent academic and pharmaceutical research accounts of pro-convulsant side effects arising from over-activation of $mGlu_5$ may represent an impediment to the development of $mGlu_5$-targeted allosteric modulators for the treatment of schizophrenia(Rook et al., 2012; Parmentier-Batteur et al., 2013). Recent reports from our laboratory comparing PAMs with ago-PAMs support the hypothesis that positive allosteric modulators of $mGlu_5$ that are devoid of intrinsic agonist activity do not carry proconvulsant and epileptogenic side effect liabilities; however, a recent publication describes an $mGlu_5$ PAM devoid of agonist activity, which

DMD Fast Forward. Published on July 2, 2013 as DOI: 10.1124/dmd.113.052084
This article has not been copyedited and formatted. The final version may differ from this version.

nevertheless carried seizure-like adverse effects in rodents(Noetzel et al., 2012; Rook et al., 2012; Parmentier-Batteur et al., 2013). The present report highlights the possibility that *in vivo* biotransformation of $mGlu_5$ PAMs may result in the CNS exposure of a potent metabolite ligand that bears noticeable switches in pharmacology and/or pharmacokinetic disposition that are distinct from its parent ligand.

Most SAR common to classes of enzyme inhibitors or receptor agonists or antagonists targeting orthosteric sites often display an intolerance with respect to structural modifications that are installed by drug metabolizing enzymes (e.g., P450s), resulting in the pharmacological deactivation of the chemotherapeutic agent. The biotransformation of allosteric receptor modulators and/or allosteric enzyme inhibitors/activators by DMEs represents an unexpected hurdle for rational drug design efforts due to the possibility of metabolism-mediated formation of active metabolites, ligands that either display pharmacology distinct from that of the parent compound or bear potent intrinsic agonist activity that exceeds that of the parent compound, as is the apparent case with VU0403602. The SAR observed in allosteric receptor modulation are sensitive to subtle, single atom modifications commonly catalyzed by so-called phase I oxidative enzymes (e.g., P450, flavin monooxygenases, aldehyde oxidase), thus oxidative metabolism could bioactivate a parent compound to a metabolite-ligand, which could attenuate or exacerbate the desired pharmacodynamic effects, seriously complicating proof-of-concept studies and/or the safety assessment of a clinical candidate. These and other related scenarios underline the importance of continued basic science development into understanding the biotransformation and metabolic fate of allosteric modulators for the potential treatment of human disease.

Authorship Contributions:

Participated in research design: Bridges, Rook, Noetzel, Morrison, Jones, Niswender, Xiang, Stauffer, Conn, Daniels.

Conducted experiments: Bridges, Rook, Noetzel, Morrison, Vinson.

Contributed new reagents or analytical tools: Zhou, Gogliotti, Lindsley, Stauffer

Performed data analysis: Bridges, Rook, Morrison, Noetzel, Xiang, Niswender, Daniels.

Wrote or contributed to the writing of the manuscript. Bridges, Rook, Noetzel, Niswender, Lindsley, Stauffer, Conn, Daniels.

DMD Fast Forward. Published on July 2, 2013 as DOI: 10.1124/dmd.113.052084
This article has not been copyedited and formatted. The final version may differ from this version.

References:

Balani SK, Miwa GT, Gan LS, Wu JT and Lee FW (2005) Strategy of utilizing in vitro and in vivo ADME tools for lead optimization and drug candidate selection. *Current topics in medicinal chemistry* **5**:1033-1038.

Balani SKZ, T.; Yang, T.J.; Liu, Z.; Bing, H.; Lee, F.W. (2002) Effective Dosing Regimen of 1-Aminobenzotriazole for Inhibition of Antipyrine Clearance in Rats, Dogs, and Monkeys. *Drug Metabolism & Disposition* **30**:1059-1062.

Conn PJ, Lindsley CW and Jones CK (2009) Activation of metabotropic glutamate receptors as a novel approach for the treatment of schizophrenia. *Trends Pharmacol Sci* **30**:25-31.

Gregory KJ, Dong EN, Meiler J and Conn PJ (2011) Allosteric modulation of metabotropic glutamate receptors: structural insights and therapeutic potential. *Neuropharmacology* **60**:66-81.

Gregory KJ, Nguyen ED, Reiff SD, Squire EF, Stauffer SR, Lindsley CW, Meiler J and Conn PJ (2013) Probing the Metabotropic Glutamate Receptor 5 (mGlu5) Positive Allosteric Modulator (PAM) Binding Pocket: Discovery of Point Mutations that Engender a "Molecular Switch" in PAM Pharmacology. *Molecular pharmacology*.

Hammond AS, Rodriguez AL, Townsend SD, Niswender CM, Gregory KJ, Lindsley CW and Conn PJ (2010) Discovery of a Novel Chemical Class of mGlu(5) Allosteric Ligands with Distinct Modes of Pharmacology. *ACS Chem Neurosci* **1**:702-716.

Kalvass JC and Maurer TS (2002) Influence of nonspecific brain and plasma binding on CNS exposure: implications for rational drug discovery. *Biopharm Drug Dispos* **23**:327-338.

Lamb JP, Engers DW, Niswender CM, Rodriguez AL, Venable DF, Conn PJ and Lindsley CW (2011) Discovery of molecular switches within the ADX-47273 mGlu5 PAM scaffold that modulate modes of pharmacology to afford potent mGlu5 NAMs, PAMs and partial antagonists. *Bioorg Med Chem Lett* **21**:2711-2714.

Lee AC, Wong RK, Chuang SC, Shin HS and Bianchi R (2002) Role of synaptic metabotropic glutamate receptors in epileptiform discharges in hippocampal slices. *J Neurophysiol* **88**:1625-1633.

Lindsley CW (2011) Molecular switches' on mGluR allosteric ligands that modulate modes of pharmacology and/or subtype selectivity., in *7th International Metabotropic Glutamate Receptors Meeting*, Taormina, Italy.

Liu X, Chen C and Smith BJ (2008) Progress in brain penetration evaluation in drug discovery and development. *The Journal of pharmacology and experimental therapeutics* **325**:349-356.

Marek GJ, Behl B, Bespalov AY, Gross G, Lee Y and Schoemaker H (2010) Glutamatergic (N-methyl-D-aspartate receptor) hypofrontality in schizophrenia: too little juice or a miswired brain? *Mol Pharmacol* **77**:317-326.

Niswender CM, Johnson KA, Weaver CD, Jones CK, Xiang Z, Luo Q, Rodriguez AL, Marlo JE, de Paulis T, Thompson AD, Days EL, Nalywajko T, Austin CA, Williams MB, Ayala JE, Williams R, Lindsley CW and Conn PJ (2008) Discovery, characterization, and antiparkinsonian effect of novel positive allosteric modulators of metabotropic glutamate receptor 4. *Mol Pharmacol* **74**:1345-1358.

Noetzel MJ, Rook JM, Vinson PN, Cho HP, Days E, Zhou Y, Rodriguez AL, Lavreysen H, Stauffer SR, Niswender CM, Xiang Z, Daniels JS, Jones CK, Lindsley CW, Weaver CD and Conn PJ (2012) Functional impact of allosteric agonist activity of selective positive

allosteric modulators of metabotropic glutamate receptor subtype 5 in regulating central nervous system function. *Mol Pharmacol* **81**:120-133.

Obach RS and Reed-Hagen AE (2002) Measurement of Michaelis constants for cytochrome P450-mediated biotransformation reactions using a substrate depletion approach. *Drug Metab Dispos* **30**:831-837.

Olney JW, Newcomer JW and Farber NB (1999) NMDA receptor hypofunction model of schizophrenia. *J Psychiatr Res* **33**:523-533.

Parmentier-Batteur S, Hutson PH, Menzel K, Uslaner JM, Mattson BA, O'Brien JA, Magliaro BC, Forest T, Stump CA, Tynebor RM, Anthony NJ, Tucker TJ, Zhang XF, Gomez R, Huszar SL, Lambeng N, Faure H, Le Poul E, Poli S, Rosahl TW, Rocher JP, Hargreaves R and Williams TM (2013) Mechanism based neurotoxicity of mGlu5 positive allosteric modulators - Development challenges for a promising novel antipsychotic target. *Neuropharmacology*.

Rodriguez AL, Grier MD, Jones CK, Herman EJ, Kane AS, Smith RL, Williams R, Zhou Y, Marlo JE, Days EL, Blatt TN, Jadhav S, Menon UN, Vinson PN, Rook JM, Stauffer SR, Niswender CM, Lindsley CW, Weaver CD and Conn PJ (2010) Discovery of novel allosteric modulators of metabotropic glutamate receptor subtype 5 reveals chemical and functional diversity and in vivo activity in rat behavioral models of anxiolytic and antipsychotic activity. *Mol Pharmacol* **78**:1105-1123.

Rook JM, Noetzel MJ, Pouliot WA, Bridges TM, Vinson PN, Cho HP, Zhou Y, Gogliotti RD, Manka JT, Gregory KJ, Stauffer SR, Edward Dudek F, Xiang Z, Niswender CM, Scott Daniels J, Jones CK, Lindsley CW and Jeffrey Conn P (2012) Unique Signaling Profiles of Positive Allosteric Modulators of Metabotropic Glutamate Receptor Subtype 5 Determine Differences in In Vivo Activity. *Biological psychiatry*.

Sharma S, Kedrowski J, Rook JM, Smith RL, Jones CK, Rodriguez AL, Conn PJ and Lindsley CW (2009) Discovery of molecular switches that modulate modes of metabotropic glutamate receptor subtype 5 (mGlu5) pharmacology in vitro and in vivo within a series of functionalized, regioisomeric 2- and 5-(phenylethynyl)pyrimidines. *Journal of medicinal chemistry* **52**:4103-4106.

Tizzano JP, Griffey KI and Schoepp DD (1995a) Induction or protection of limbic seizures in mice by mGluR subtype selective agonists. *Neuropharmacology* **34**:1063-1067.

Tizzano JP, Griffey KI and Schoepp DD (1995b) Receptor subtypes linked to metabotropic glutamate receptor agonist-mediated limbic seizures in mice. *Ann N Y Acad Sci* **765**:230-235; discussion 248.

Tsai G and Coyle JT (2002) Glutamatergic mechanisms in schizophrenia. *Annu Rev Pharmacol Toxicol* **42**:165-179.

Vinson PN and Conn PJ (2012) Metabotropic glutamate receptors as therapeutic targets for schizophrenia. *Neuropharmacology*.

Williams R, Manka JT, Rodriguez AL, Vinson PN, Niswender CM, Weaver CD, Jones CK, Conn PJ, Lindsley CW and Stauffer SR (2011) Synthesis and SAR of centrally active mGlu5 positive allosteric modulators based on an aryl acetylenic bicyclic lactam scaffold. *Bioorganic & medicinal chemistry letters* **21**:1350-1353.

Wong RK, Bianchi R, Chuang SC and Merlin LR (2005) Group I mGluR-induced epileptogenesis: distinct and overlapping roles of mGluR1 and mGluR5 and implications for antiepileptic drug design. *Epilepsy Curr* **5**:63-68.

Wood MR, Hopkins CR, Brogan JT, Conn PJ and Lindsley CW (2011) "Molecular switches" on mGluR allosteric ligands that modulate modes of pharmacology. *Biochemistry* **50**:2403-2410.

Zhao W, Bianchi R, Wang M and Wong RK (2004) Extracellular signal-regulated kinase 1/2 is required for the induction of group I metabotropic glutamate receptor-mediated epileptiform discharges. *J Neurosci* **24**:76-84.

Footnotes:

This work was supported by the National Institutes of Health [Grants R01-MH062646, R01-MH074953, and U01-MH087965]. Portions of this work were presented at the North American Meetings of the International Society for the Study of Xenobiotics, October 2012, Dallas, TX.

DMD Fast Forward. Published on July 2, 2013 as DOI: 10.1124/dmd.113.052084
This article has not been copyedited and formatted. The final version may differ from this version.

Legends for Schemes and Figures:

Scheme 1. Principal pathways of VU0403602 metabolism observed *in vitro* in male Sprague-Dawley rat hepatic S9 fractions.

Figure 1. Structures of $mGlu_5$ allosteric modulators.

Figure 2. VU0403602 is a potent positive allosteric modulator of $mGlu_5$ with direct agonist activity in the absence of glutamate *in vitro*. VU0403602 causes concentration-dependent increases in the mobilization of intracellular calcium in recombinant cells expressing $mGlu_5$ in the presence (top) and absence (bottom) of a fixed submaximal (~EC_{20}) concentration of glutamate, and with a PAM EC_{50} of 4 nM (100 % response achieved relative to the maximal response obtained with glutamate, % Glu_{max}) and an agonist EC_{50} of 31.1 nM (49.4 % Glu_{max}). Data represent the mean ± SEM of four independent experiments performed in duplicate.

Figure 3. The $mGlu_5$ ago-PAM VU0403602 induces time-dependent increases in behavioral convulsions, which are mitigated by pre-treatment with the $mGlu_5$ antagonist MPEP or the P450 inactivator ABT in male Sprague-Dawley rats. VU0403602 administration (IP, 30 mg/kg, $N = 9$) causes full clonic/tonic seizure activity (modified Racine score 5), while the same administration of VU0403602 to rats pre-treated with a lower dose of MPEP (IP, 5 mg/kg, $N = 3$) or a higher dose of MPEP (IP, 10 mg/kg, $N = 3$) reduced (modified racine score 2) or completely blocked (modified racine score 0), respectively, the severity of seizure activity. In rats pre-treated with

DMD Fast Forward. Published on July 2, 2013 as DOI: 10.1124/dmd.113.052084
This article has not been copyedited and formatted. The final version may differ from this version.

ABT (PO, 50 mg/kg, *N* = 6), administration of VU0403602 (IP, 30 mg/kg) failed to induce any seizure activity (modified racine score 0). Data represent mean ± SEM.

Figure 4. Representative reconstructed LC/MS/MS total ion current (TIC; **A**) of extracts from a Rat hepatic S9 incubation (+NADPH) of VU0403602, showing the principal metabolites **M1** and **M2**, as well as a minor hydroxylated metabolite **M3**. A corresponding TIC (**B**) from the LC/MS/MS analysis (MS/MS, *m/z* 311) of brain extracts from rats receiving a 30 mg/kg dose (IP) of VU0403602 reveals **M1** to be the principal hydroxylated metabolite *in vivo*.

Figure 5. M1 is a potent positive allosteric modulator of $mGlu_5$ with direct agonist activity in the absence of glutamate *in vitro*. **M1** causes concentration-dependent increases in the mobilization of intracellular calcium in recombinant cells expressing $mGlu_5$ in the presence (top) and absence (bottom) of a fixed submaximal (~EC_{20}) concentration of glutamate, and with a PAM EC_{50} of 16.9 nM (94 % Glu_{max}) and an agonist EC_{50} of 400 nM (79 % Glu_{max}). Data represent the mean ± SEM of at least three independent experiments performed in duplicate.

Figure 6. VU0403602 and **M1 (**VU0453103) induce long-term depression at the Schaffer collateral-CA1 synapse in hippocampus. A stimulus that produced a 50-60% fEPSP slope was used as baseline stimulation for each recording. Bath application of 75 μM DHPG for 10 minutes (solid line) induced LTD that lasted at least 55 minutes after washout (*N* = 8). Similarly, bath application of either 10 μM VU0403602 or 10 μM **M1** for 10 minutes (solid line) resulted in LTD that lasted at least 55 minutes after washout of the compound (*N* = 8, 7 respectively).

DMD Fast Forward. Published on July 2, 2013 as DOI: 10.1124/dmd.113.052084
This article has not been copyedited and formatted. The final version may differ from this version.

Insets are sample traces measured predrug (black) or 55 minutes after compound washout (grey). Data represent mean ± SEM.

Figure 7. VU0403602 and **M1** (VU0453103) induce epileptiform activity in CA3 neurons in hippocampus. Amplitude and inter-event interval of spontaneous firing were determined using field potential recordings in CA3 in the hippocampal formation. A) Application of 50 μM DHPG (N = 11), 10 μM VU0403602 (N = 8) or 10 μM **M1** (N = 7) for 10 minutes resulted in a robust decrease in the inter-event interval of spontaneous events, while having no significant effect on amplitude of spontaneous events. Data represent mean ± SEM. B)
Sample traces from individual experiments taken pre and post compound addition.

Figure 8. The $mGlu_5$ ago-PAM metabolite **M1** induces dose- and time- dependent increases in behavioral adverse effects in male Sprague-Dawley rats receiving a single administration (IP, 30 mg/kg, N = 2), while the inactive metabolite **M2** is devoid of adverse effects (IP, 30 mg/kg, N = 2). Data represent mean ± SEM.

DMD Fast Forward. Published on July 2, 2013 as DOI: 10.1124/dmd.113.052084
This article has not been copyedited and formatted. The final version may differ from this version.

Tables:

Table 1. Pharmacokinetics of VU0403602 and the formation of its principle metabolites (**M1**, **M2**) in vivo in male Sprague-Dawley rats following intraperitoneal (IP) administration (30 mg/kg) in the absence and presence of pre-treatment with the P450 inactivator 1-aminobenzotriazole (ABT). Data represent mean values ($N = 2$).

Analyte	Pretreatment	Plasma C_{max} µM	Plasma T_{max} hr	Plasma $AUC_{0\text{-}inf}$ µM*hr	Brain C_{max} µM	Brain $AUC_{0\text{-}inf}$ µM*hr
VU0403602	-	3.21 (0.005)[a]	0.25	3.63 (0.006)[a]	11.5 (0.006)[b]	7.79 (0.004)[b]
	+ABT	11.0 (0.018)[a]	0.75	9.64 (0.015)[a]	12.9 (0.006)[b]	9.64 (0.005)[b]
M1	-	0.064 (0.004)[c]	1.5	0.046 (0.003)[c]	0.406 (0.005)[d]	0.258 (0.003)[d]
	+ABT	0.032 (0.002)[c]	1.5	0.003 (0.001)[c]	0.031 (0.001)[d]	0.031 (0.001)[d]
M2[e]	-	17.8	1.25	15.8	3.71	3.15
	+ABT	20.3	1.5	11.7	6.73	4.25

[a](unbound concentrations), Fu 0.0016; [b]nonspecific binding, $f_u < 0.005$

[c](unbound concentrations), Fu 0.06; [d]nonspecific binding f_u 0.011

[e]unbound concentrations for M2 not determined

Scheme 1

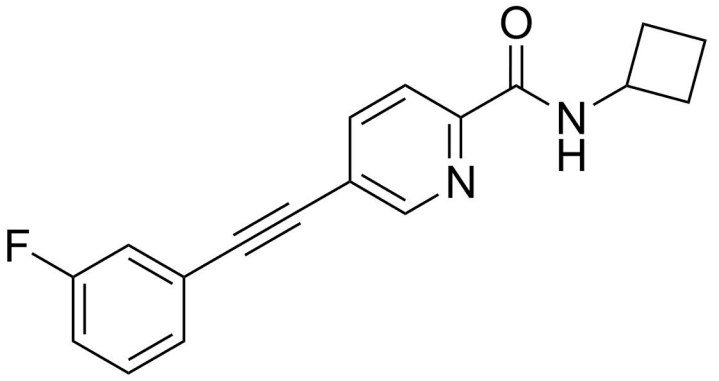

VU0403602

P450

hydrolysis

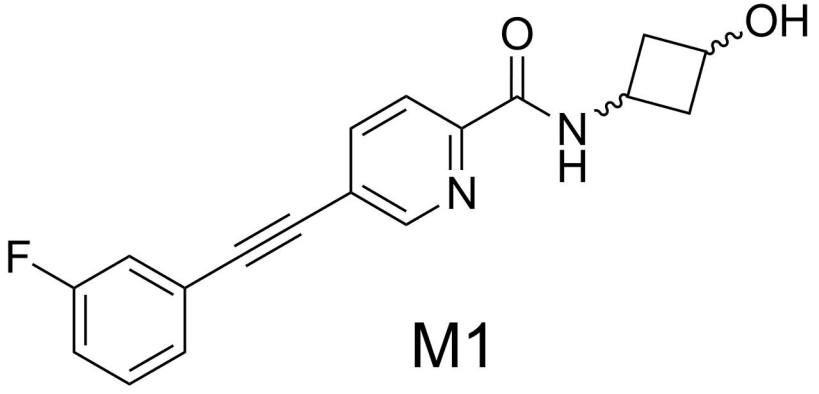

M1

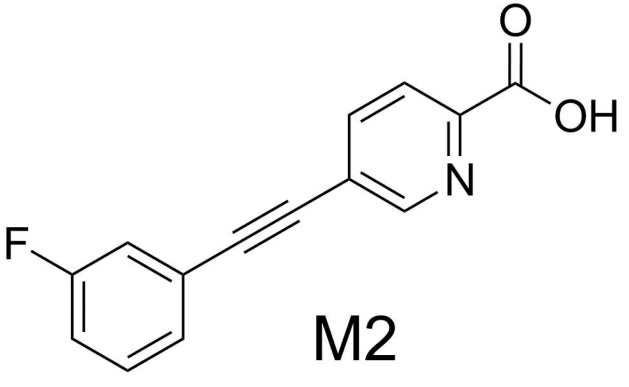

M2

Figure 1

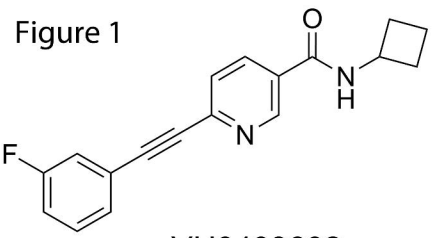

VU0403602

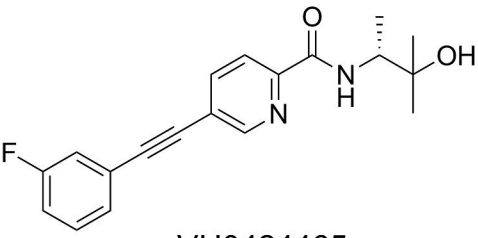

VU0424465

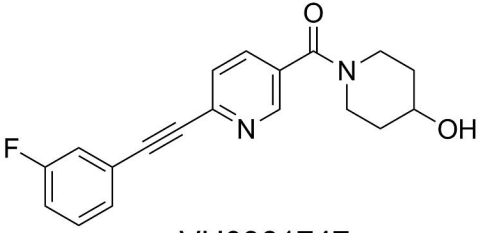

VU0361747

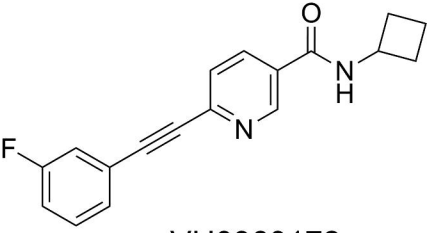

VU0360172

Figure 2

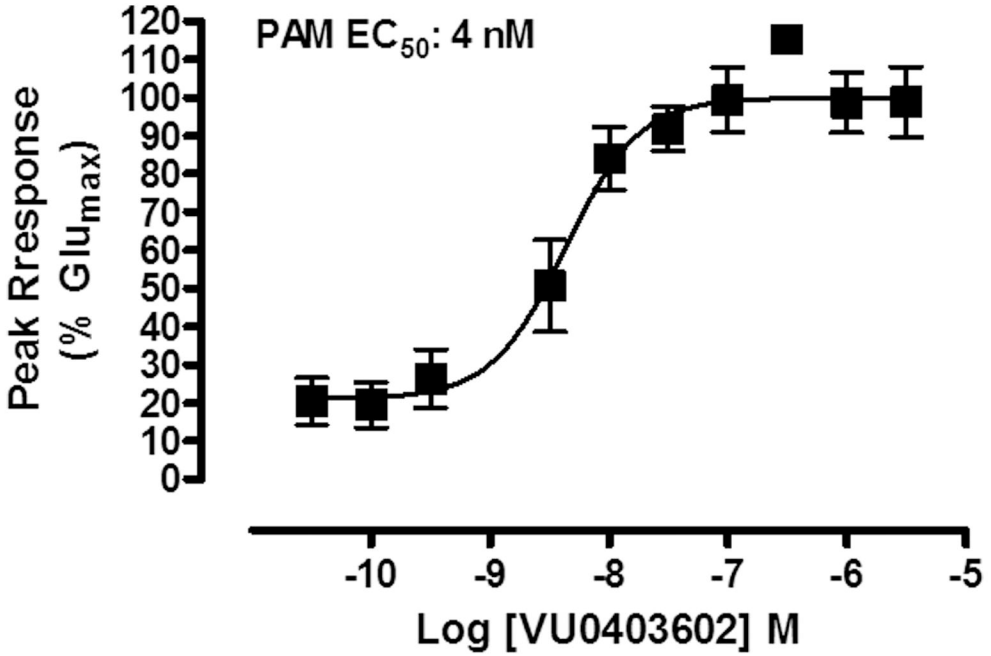
PAM EC50: 4 nM
Peak Rresponse
(% Glumax)
120
110
100
90
80
70
60
50
40
30
20
10
0
-10
-9
-8
-7
-6
-5
Log [VU0403602] M

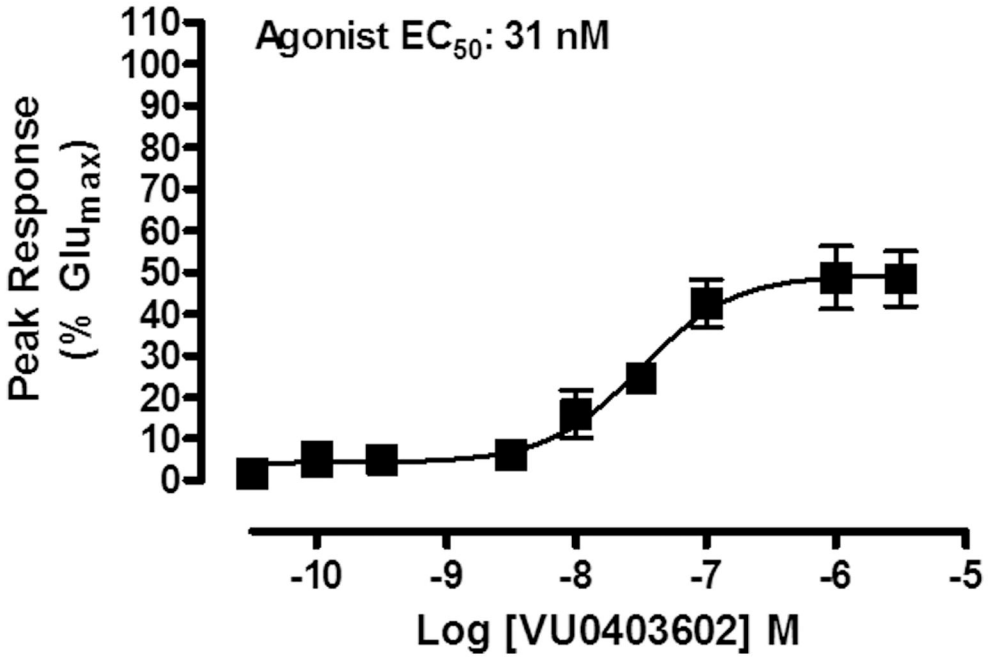
Agonist EC50: 31 nM
Peak Response
(% Glumax)
110
100
90
80
70
60
50
40
30
20
10
0
-10
-9
-8
-7
-6
-5
Log [VU0403602] M

Figure 3

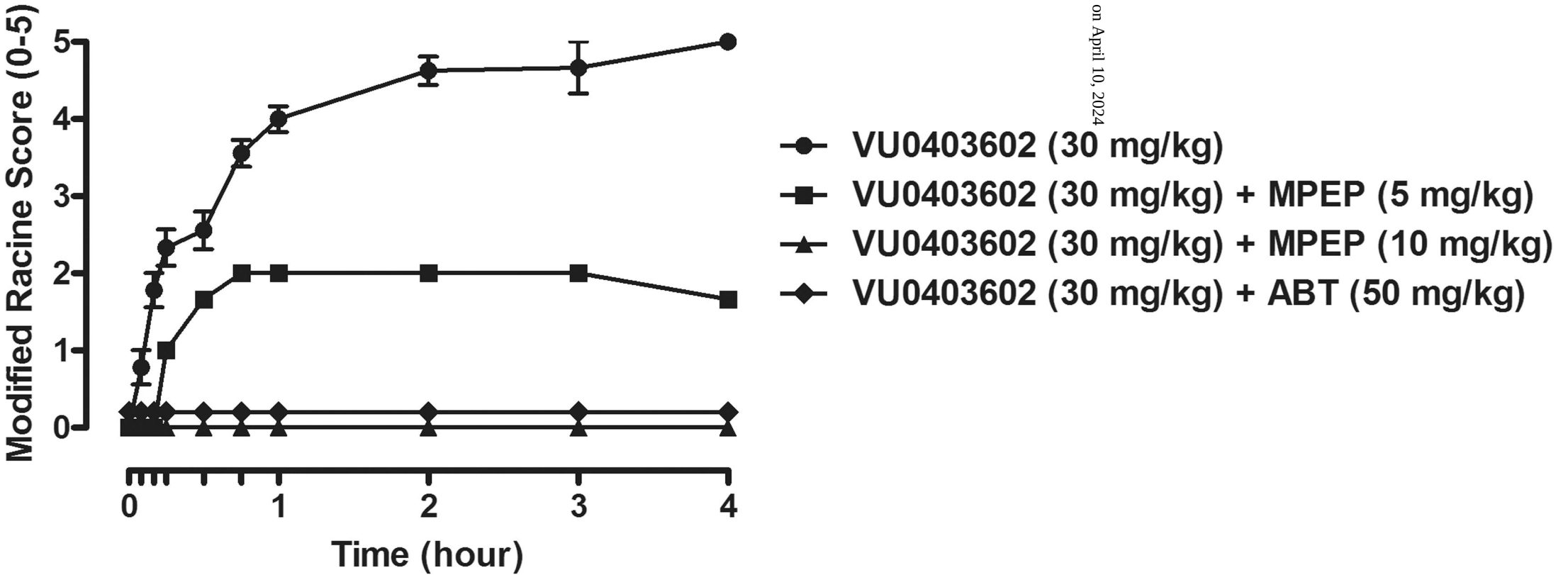

Figure 4

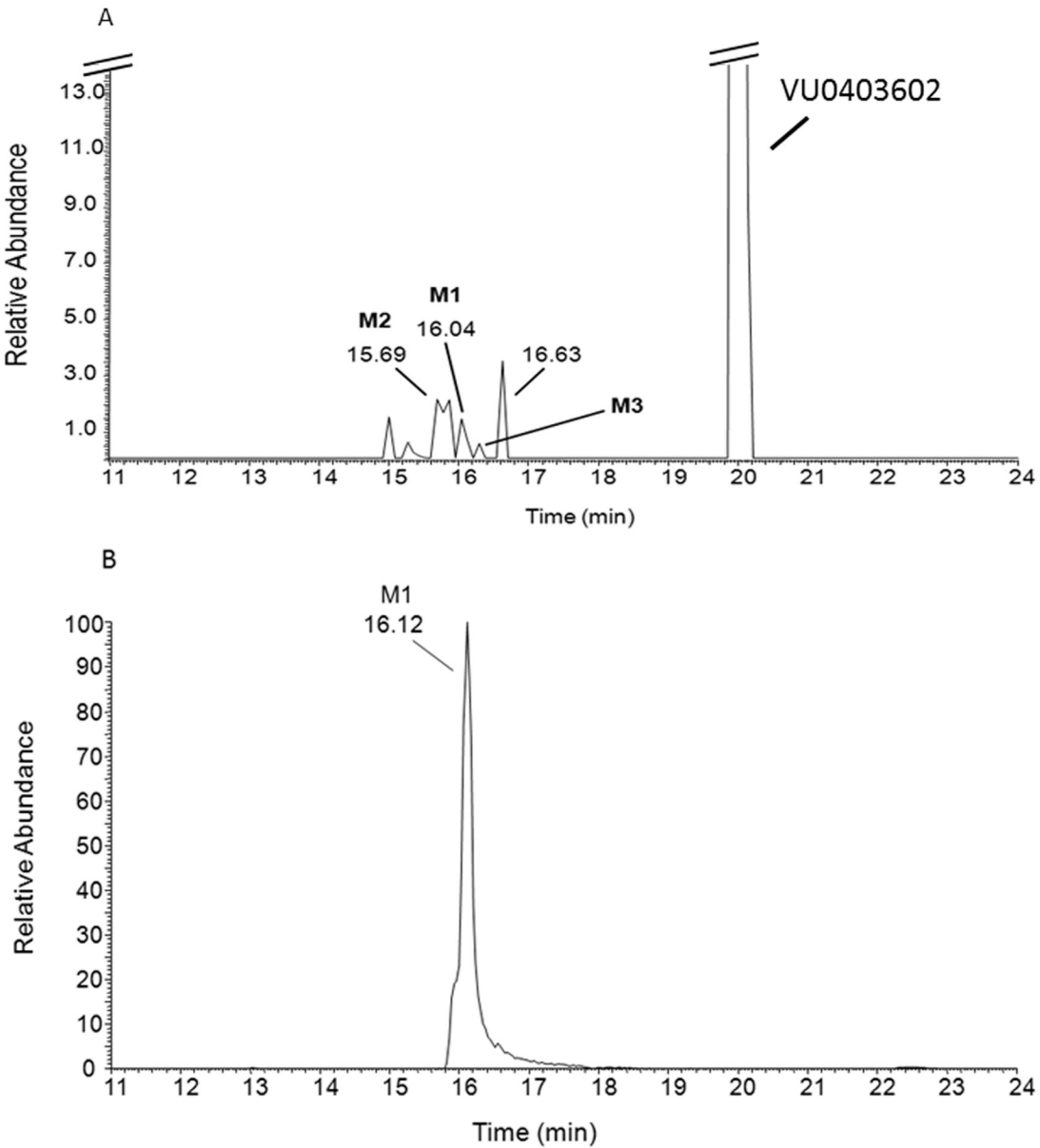
A
VU0403602
M1
16.04
M2
15.69
16.63
M3
Relative Abundance
Time (min)
B
M1
16.12
Relative Abundance
Time (min)

Figure 5

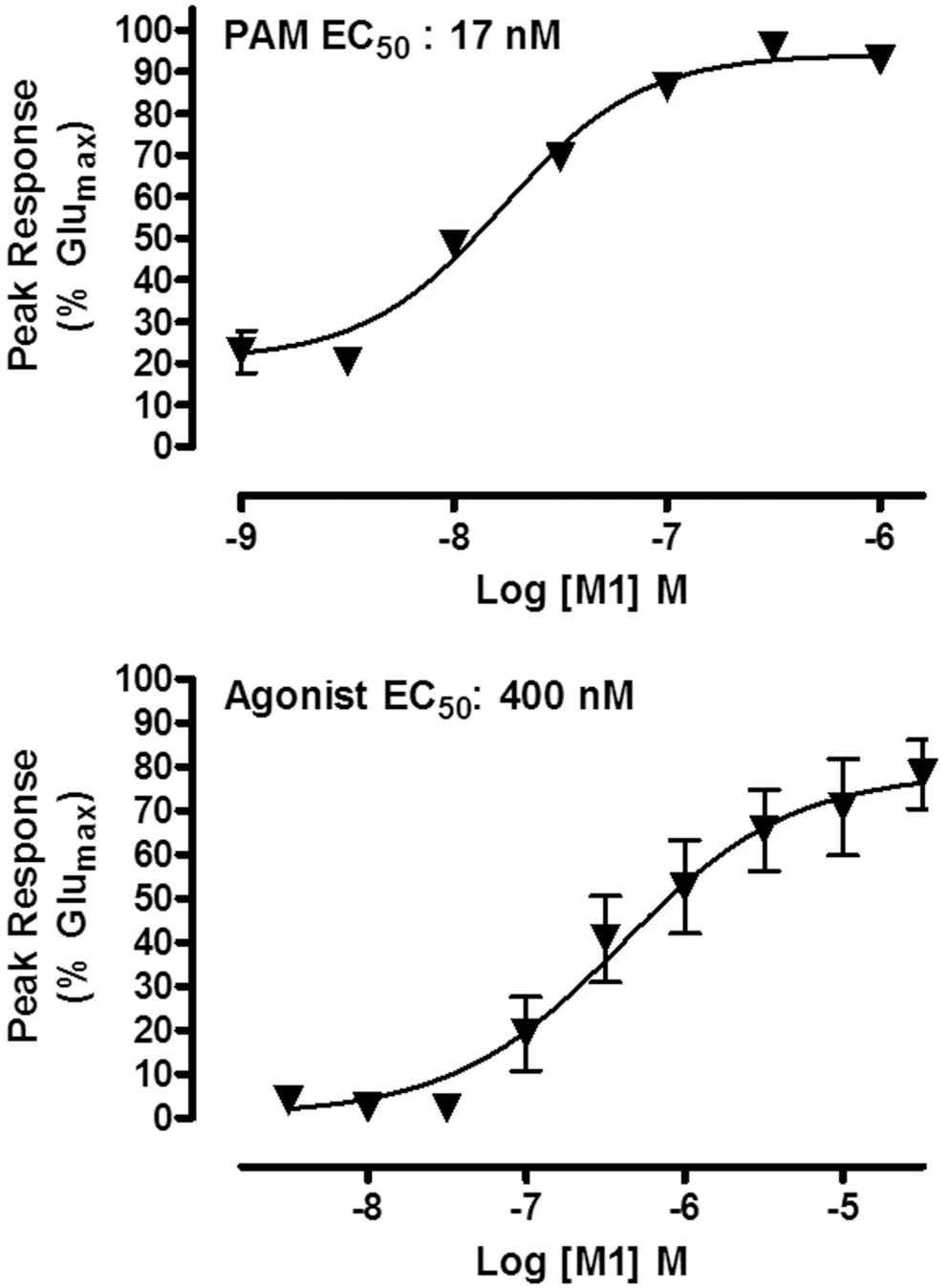
PAM EC50 : 17 nM
Peak Response
(% Glumax)
100
90
80
70
60
50
40
30
20
10
0
-9
-8
-7
-6
Log [M1] M
Agonist EC50: 400 nM
Peak Response
(% Glumax)
100
90
80
70
60
50
40
30
20
10
0
-8
-7
-6
-5
Log [M1] M

Figure 6

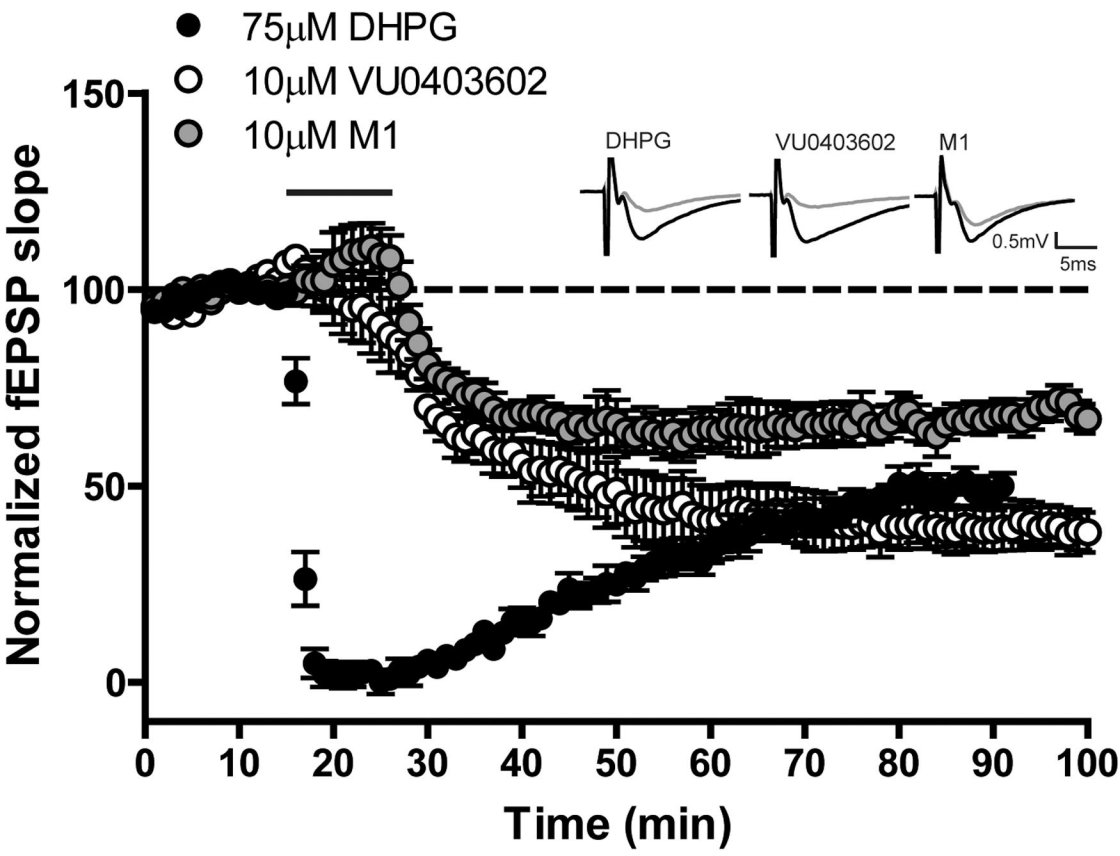
75μM DHPG
10μM VU0403602
10μM M1
DHPG
VU0403602
M1
0.5mV
5ms
Normalized fEPSP slope
150
100
50
0
0
10
20
30
40
50
60
70
80
90
100
Time (min)

Figure 7

A

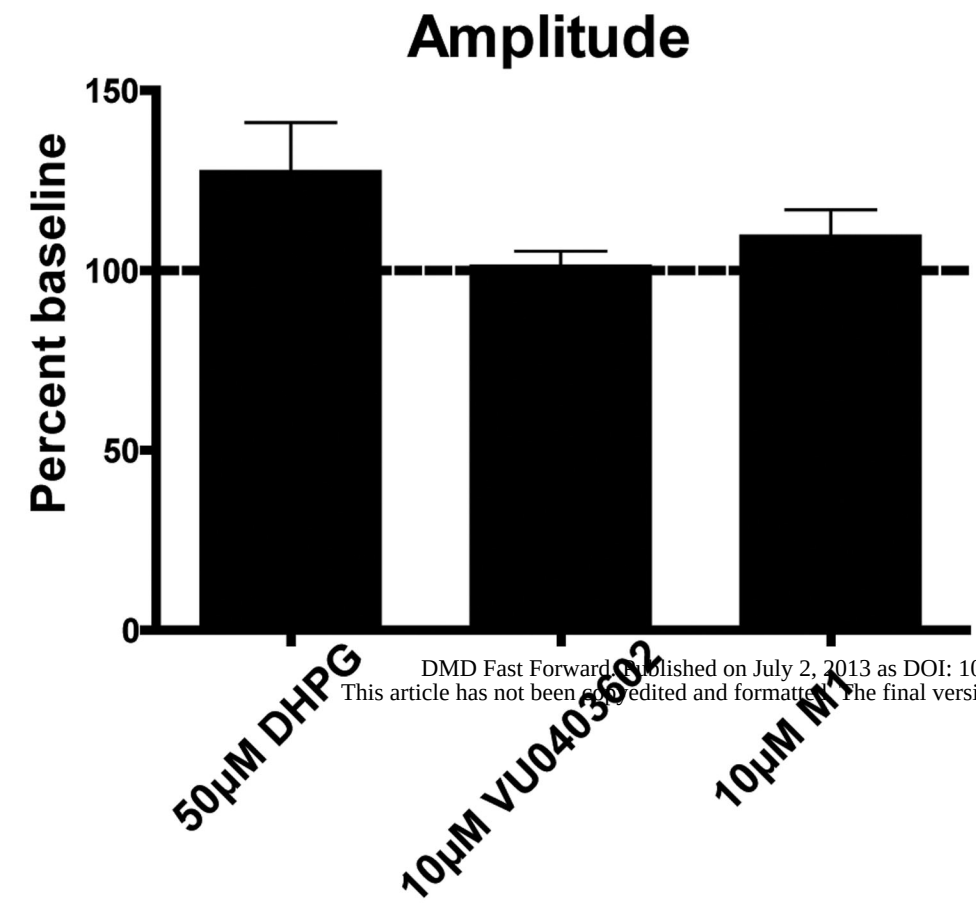

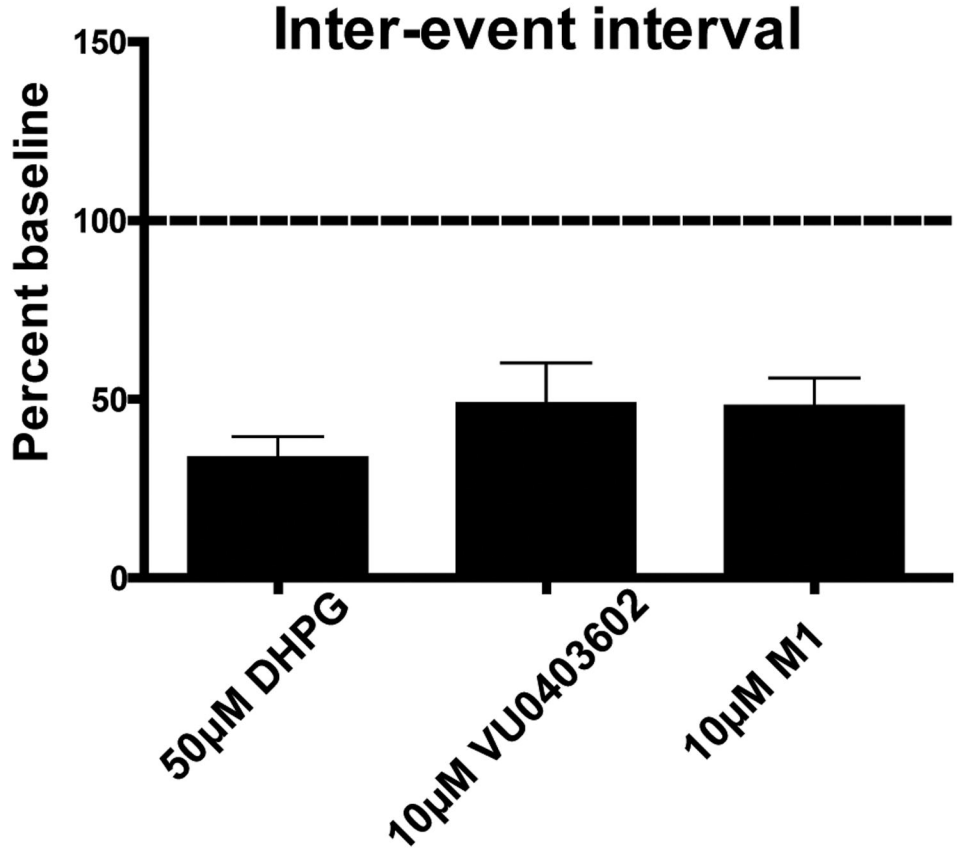

B

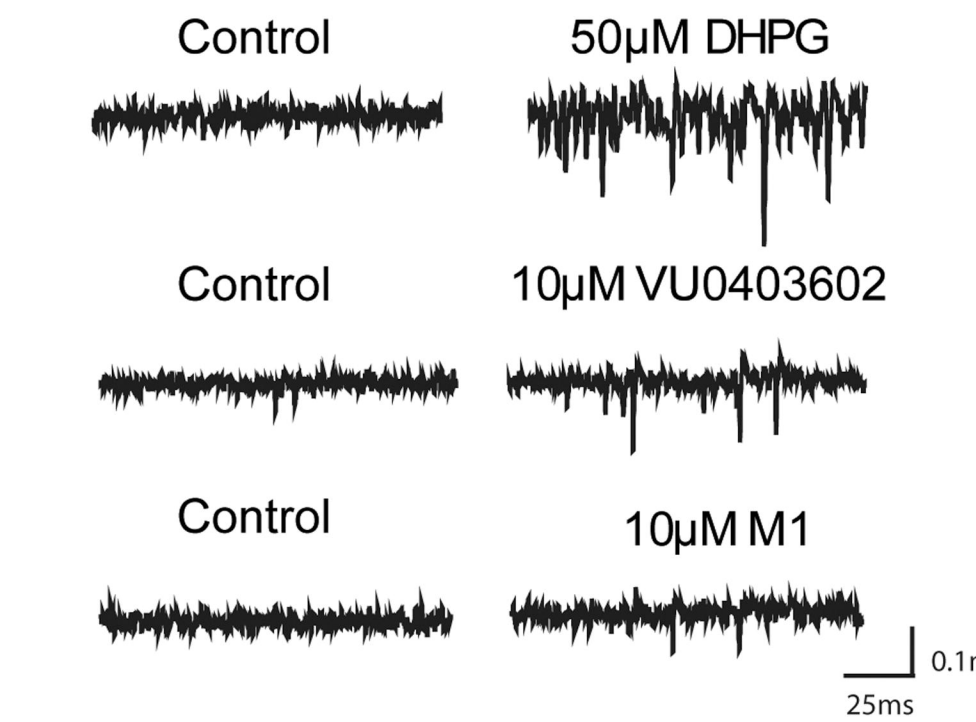

Figure 8

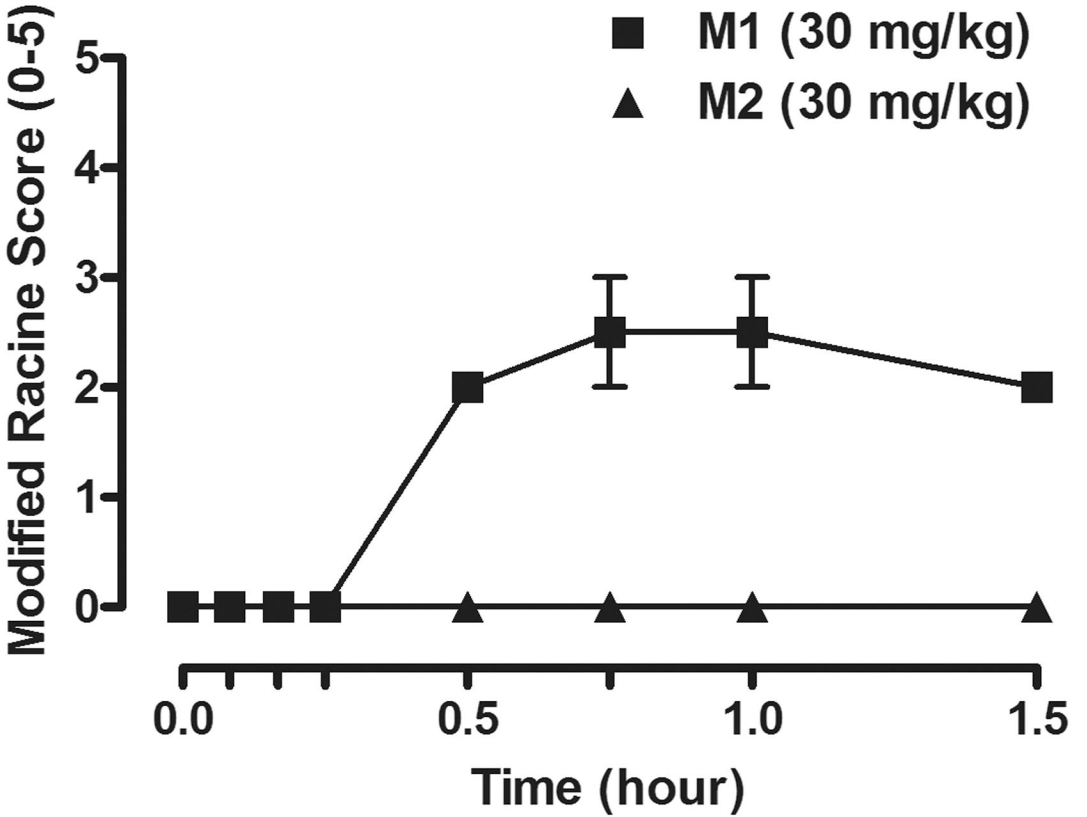
M1 (30 mg/kg)
M2 (30 mg/kg)
Modified Racine Score (0-5)
5
4
3
2
1
0
0.0
0.5
1.0
1.5
Time (hour)

Supplemental Information

Biotransformation of a Novel Positive Allosteric Modulator of Metabotropic Glutamate Receptor Subtype 5 Contributes to Seizure-Like Adverse Events in Rats Involving a Receptor Agonism-Dependent Mechanism

(Journal: Drug Metabolism & Disposition)

Thomas M. Bridges, Jerri M. Rook, Meredith J. Noetzel, Ryan D. Morrison, Ya Zhou, Rocco D. Gogliotti, Paige N. Vinson, Zixiu Xiang, Carrie K. Jones, Colleen M. Niswender, Craig W. Lindsley, Shaun R. Stauffer, P. Jeffrey Conn, J. Scott Daniels

Vanderbilt Center for Neuroscience Drug Discovery, Department of Pharmacology (T.M.B., R.D.M., J.S.D. J.M.R., M.J.N., P.N.V., Z.X., C.M.N., P.J.C. C.K.J. C.W.L., S.R.S.), Department of Chemistry (C.W.L.),Vanderbilt University Medical Center, Nashville, TN 37232-6600, USA

Chemical Synthesis

Scheme 1

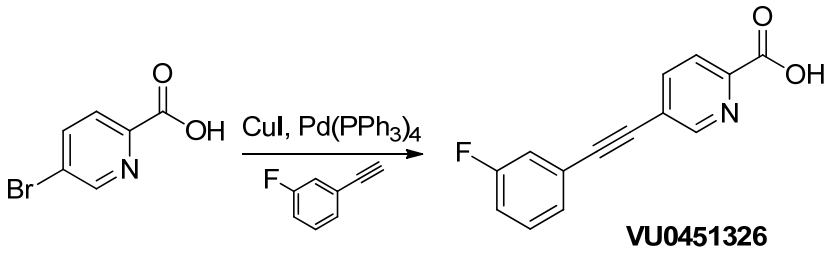

5-((3-fluorophenyl)ethynyl)picolinic acid (VU0451326): 5-bromopicolinic acid (2.0 g, 10 mmol) was combined in a microwave vial with 1-ethynyl-3-fluorobenzene (1.03 mL, 12 mmol), tetrakis(triphenylphosphine) palladium (0) (0.57 g, 0.5 mmol), copper iodide (0.19 g, 1.0 mmol), diethylamine (6.2 mL, 60 mmol), and DMF (15 mL). The reaction was subjected to microwave irradiation for 45 min at 90°C. The reaction was diluted with EtOAc (90 mL) and extracted with H_2O (90 mL). The aqueous layer was separated and acidified with HCl (4M aqueous) until pH ~ 2. A white precipitate formed and was filtered to pure afford **VU0451326** (1.71 g, 71%): ^{1}H NMR (400 MHz, MeOH) δ 8.82 (s, 1H), 8.21-8.12 (m, 2H), 7.49-7.43 (m, 2H), 7.39-7.32 (m, 1H), 7.24-7.19 (m, 1H). LC/MS (>98%), 0.696 min, *m/z* = 242.1 [M+H]; HRMS = 242.0615 [M+H], calculated for $C_{14}H_8FNO_2$, 242.0617.

Scheme 2

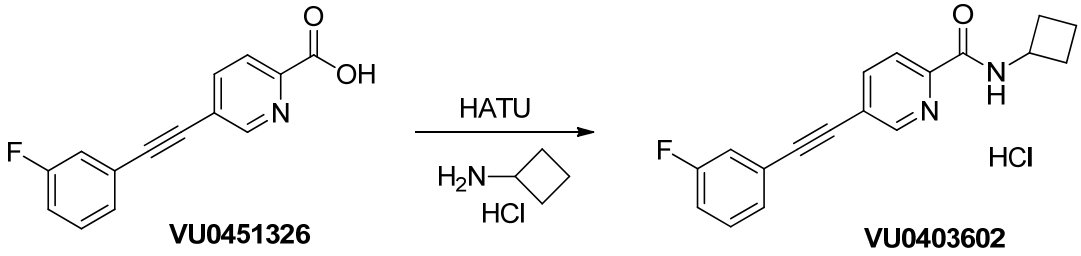

N-cyclobutyl-5-((3-fluorophenylethynyl)picolinamide (VU0403602): To a solution of 5-((3-fluorophenyl)ethynyl)picolinic acid (**VU0451326**, 1.29 g, 5.0 mmol) in DMF (20 mL) was added HATU (2.28 g, 6.0 mmol), cyclobutanamine hydrochloride (0.645 g, 6.0 mmol), and diisopropylethylamine (3.48 mL, 20.0 mmol). The reaction stirred at room temperature until LC/MS showed complete consumption of starting material. The reaction was quenched with H_2O (60 mL) and extracted with EtOAc (60 mL x 3). The combined organics were dried over $MgSO_4$ and concentrated under reduced pressure. The crude material was purified by silica gel column chromatography (0-30% EtOAc/Hexanes). The pure free base compound was dissolved in dioxane (5 mL) and cooled to 0°C. To the solution was added 4M HCl (4mL, 16 mmol). A white precipitate formed and was filtered and dried *in vacuo* to give **VU0403602** as an HCl salt: ^{1}H NMR (400 MHz, DMSO) δ 9.03 (d, *J* = 8.4 Hz, 1H), 8.83 (s, 1H), 8.19-8.16 (dd, *J* = 6.0, 2.0 Hz, 1H), 8.06 (d, *J* = 8.0 Hz, 1H), 7.56-7.48 (m, 3H), 7.38-7.33 (m, 1H), 4.51-4.43 (m, 1H), 2.22-2.16 (m, 4H), 1.70-1.64 (m, 2H); LC/MS (>98%), 3.78 min, *m/z* = 295.1 [M+H]; HRMS = 317.1066 [M+Na], calculated for $C_{18}H_{15}FN_2ONa$, 317.1066.

Scheme 3

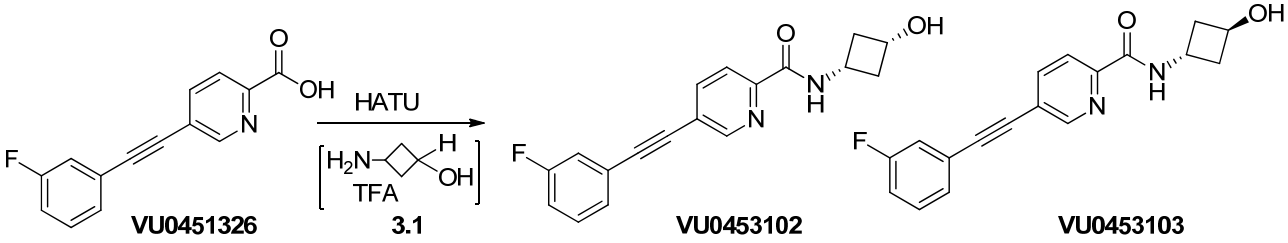

3-aminocyclobutanol 2,2,2-trifluoroacetate (3.1): To a 0°C solution of *tert*-butyl(3-oxocyclobutyl)carbamate (370 mg, 2.0 mmol) in THF (15 mL) was added sodium borohydride (91 mg, 2.4 mmol). LC/MS indicated complete conversion of starting material after 1.5 h. The

reaction was carefully quenched with sodium hydroxide solution (200 mg in 1mL H_2O). The organic layer was separated, dried over $MgSO_4$, and concentrated under reduced pressure. The crude product was dissolved in DCM (15 mL) and trifluoroacetic acid (5 mL) was slowly added. The mixture was allowed to stir for 1h and the mixture concentrated under reduced pressure. The crude residue was further dried *in vacuo* to afford **3.1** (320 mg, 80%) as a TFA salt. The amine was used directly in the next step without further purification.

5-((3-fluorophenyl)ethynyl)-N-(3-hydroxycyclobutyl)picolinamide) (VU0453102, VU0453103): To a solution of 5-((3-fluorophenyl)ethynyl)picolinic acid (231 mg, 0.96 mmol) in DMF (5 mL) was added HATU (438 mg, 1.15 mmol). The mixture stirred at room temperature for 30 min. To the reaction was added **3.1** (160 mg, 0.8 mmol) and diethylamine (0.5 mL, 2.88 mmol). The mixture stirred at room temperature for 1h when LC/MS indicated full conversion of starting material to product. The reaction was quenched with H_2O (20 mL) and extracted with EtOAc (20 mL x 3). The crude mixture was purified by silica gel column chromatography (0-5% MeOH/DCM) to afford 240 mg (82% yield) of a *cis*/*trans* of the title compound as a white powder. Separation of the *cis*/*trans* mixture was accomplished using a supercritical fluid chromatography (SFC) system from THarSFC^{TM} (UV 280 nm detection). A Lux Cellulose-2 column (5 μm, 4.6 x 250 mm, Phenomenex, temp = 42 ^{o}C) was utilized using 30% MeOH (0.1% diethylamine) in CO_2 as eluent with a 5 mL/min flowrate. The first peak (Rt = 2.14 min) and second peak (Rt = 2.88 min) were individually collected, concentrated under reduced pressure and dried in vacuo to afford each respective isomer as a white solid. Peak A (first eluting peak) was collected and assigned **VU0453102** (130 mg); peak B (second eluting peak) was assigned as **VU0453103** (76 mg): ^{1}H NMR (400 MHz, C_6D_6) *cis*-**VU0453102** δ 8.78

(br s, 1H), 8.28 (d, *J* = 8.0, 1H), 8.02 (d, *J* = 7.2, NH), 7.42-7.40 (dd, *J* = 6.4, 1.6, 1H), 7.27-7.19 (m, 2H), 6.88-6.81 (m, 2H), 4.22-4.12 (m, 1H), 3.70-3.63 (m, 1H), 2.63-2.57 (m, 2H), 1.79-1.72 (m, 2H), 0.78 (s, 1H); LC/MS (>98%), 0.711 min, *m/z* = 311.0 [M+H]; HRMS = 311.1198 [M+H], calculated for $C_{18}H_{16}FN_2O_2$, 311.1196; ^{1}H NMR (400 MHz, C_6D_6) *trans*-**VU0453103** δ 8.60 (d, *J* = 1.6 Hz, 1H), 8.19 (d, *J* = 8.0 Hz, 1H), 7.91 (d, *J*= 6.8 Hz, 1H), 7.32-7.30 (dd, *J* = 6.4, 1.6 Hz, 1H), 7.14-7.10 (m, 2H), 6.77-6.62 (m, 2H), 4.78-4.69 (m, 1H), 3.98-3.93 (m, 1H), 2.13-2.06 (m, 2H), 1.97-1.91 (m, 2H), 1.05 (d, *J* = 2.4 Hz, 1H); LC/MS (>98%), 0.720 min, *m/z* = 311.0 [M+H]; HRMS = 311.1194 [M+H], calculated for $C_{18}H_{16}FN_2O_2$, 311.1196. Chemical shift analysis in addition NOE studies support the isomer A as *cis*-**VU0453102** and isomer B as *trans*-**VU0453103.**

Supplemental Figures

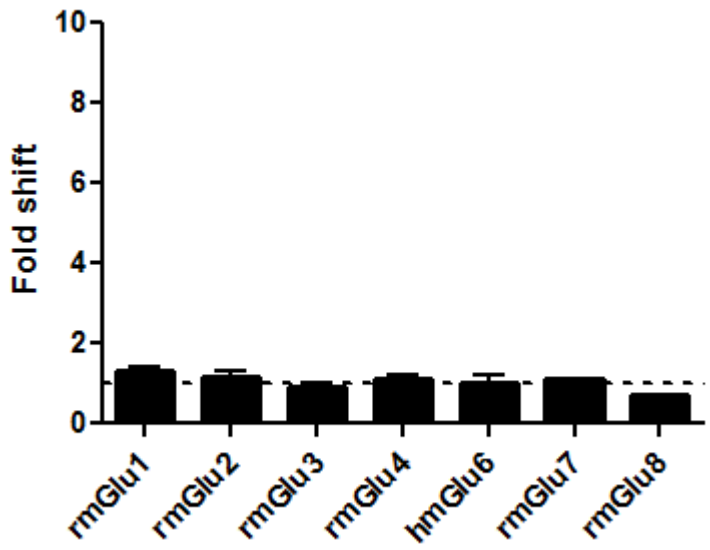

Figure S1. VU0403602 is selective for $mGlu_5$. VU0403602 was assessed for modulation of orthosteric agonist activity at $mGlu_{1\text{-}4,\ 6\text{-}8}$. Data represent the average fold shift in the glutamate concentration response induced by VU0403602 in two independent experiments (*N*=2 each).

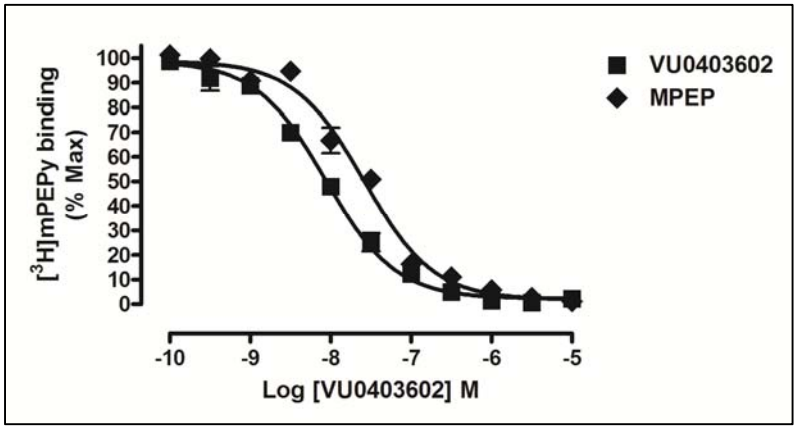

Figure S2. VU0403602 exhibits concentration-dependent inhibition of [^{3}H]mPEPy binding to membranes prepared from rat $mGlu_5$-expressing HEK293A cells. The affinity and degree of inhibition by VU0403602 (K_i = 5.18 ± 0.13 nM) was similar to that of an unlabeled MPEP control (K_i = 13.9 ± 1.42 nM). Data represent means ± SEM (*N* = 3).

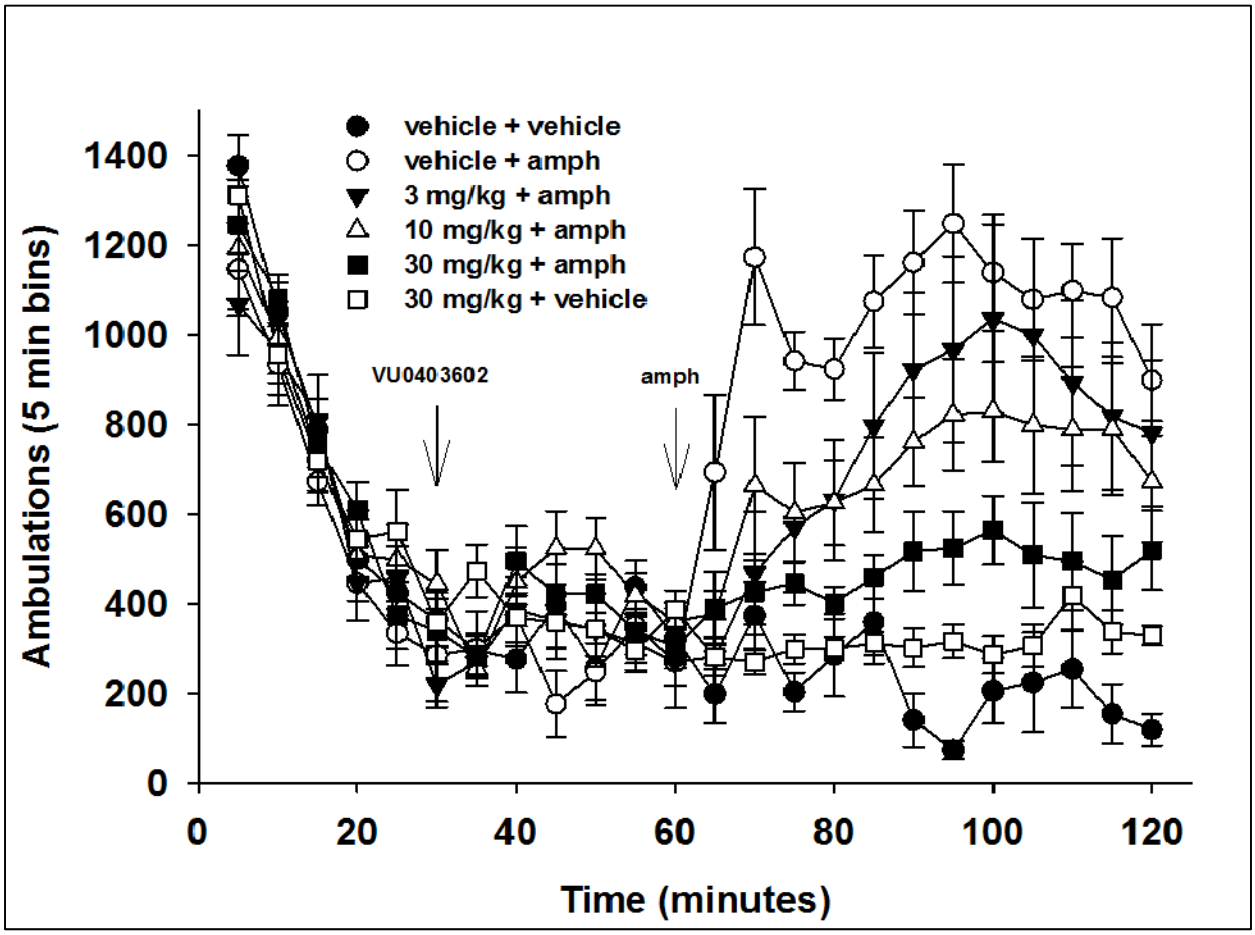

Figure S3. The $mGlu_5$ ago-PAM VU0403602 dose-dependently reverses amphetamine-induced hyperlocomotor activity in male Sprague-Dawley rats. Treatment of rats with 3, 10, or 30 mg/kg of VU0403602 reduced the area-under-the-effect-curve by 33.2, 30.6, and 63.7 %, respectively, when normalized to that of vehicle-treated rats receiving amphetamine alone (ED_{50}, 21 mg/kg). Data represent mean ± SEM (N = 8 per dose group).

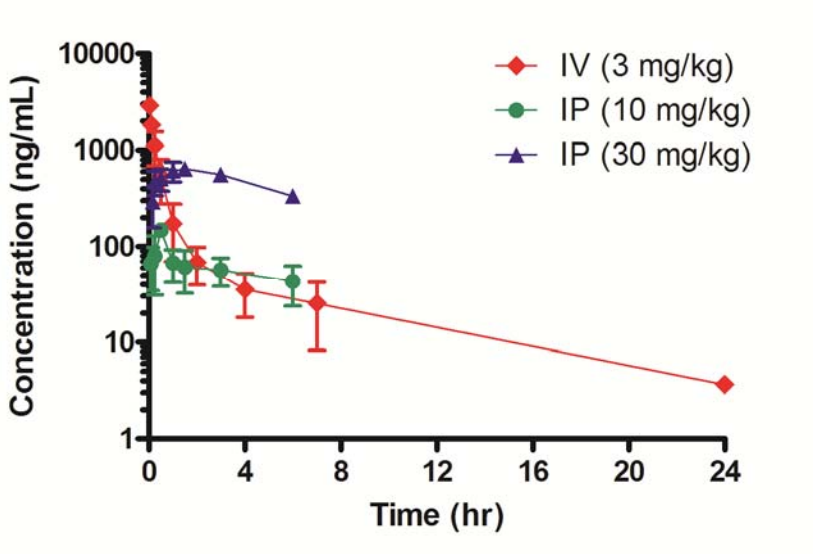

Figure S4. Plasma pharmacokinetics of $mGlu_5$ ago-PAM VU0403602 following intravenous administration (3 mg/kg, *N* = 2) to male Sprague–Dawley (SD) rats. VU0403602 exhibited moderate average clearance (36.2 mL/min/kg), large average volume of distribution at steady-state (6.73 L/kg), and a moderate average mean residence time (3.07 hr). Following a 10 mg/kg IP administration to SD Rats (*N*=3), VU0403602 reached a maximal plasma concentration (C_{max}) of 149 ng/mL. The mean exposure ($AUC_{0\text{-}last}$) of VU0403602 was 365 ng*hr/mL, resulting in an IP bioavailability of 7.5% (F=0.075). Upon increasing the IP dose of VU0403602 to 30 mg/kg, the C_{max} observed increased to 643 ng/mL, with a corresponding increase in the $AUC_{0\text{-}last}$ to 2996 ng*hr/mL. The apparent IP bioavailability at 30 mg/kg was 21% (F=0.21).

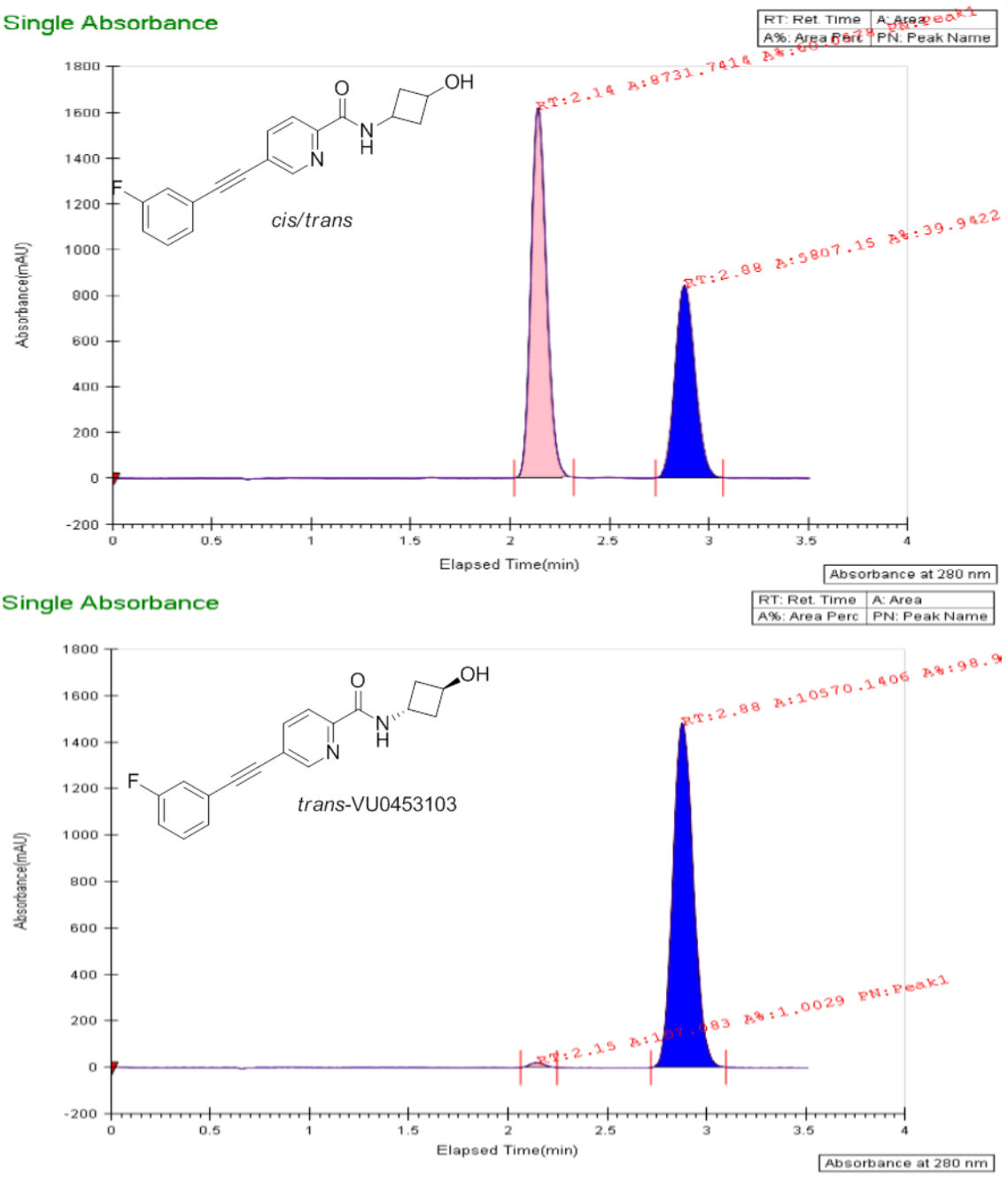

Figure S5. Analytical SFC chromatogram of *cis*/*trans* mixture (top panel) and purified eluting isomer/peak B (**VU0453103,** 5-((3-fluorophenyl)ethynyl)-N-(*trans*-3-hydroxycyclobutyl)picolinamide) retention time = 2.88 min (bottom panel).

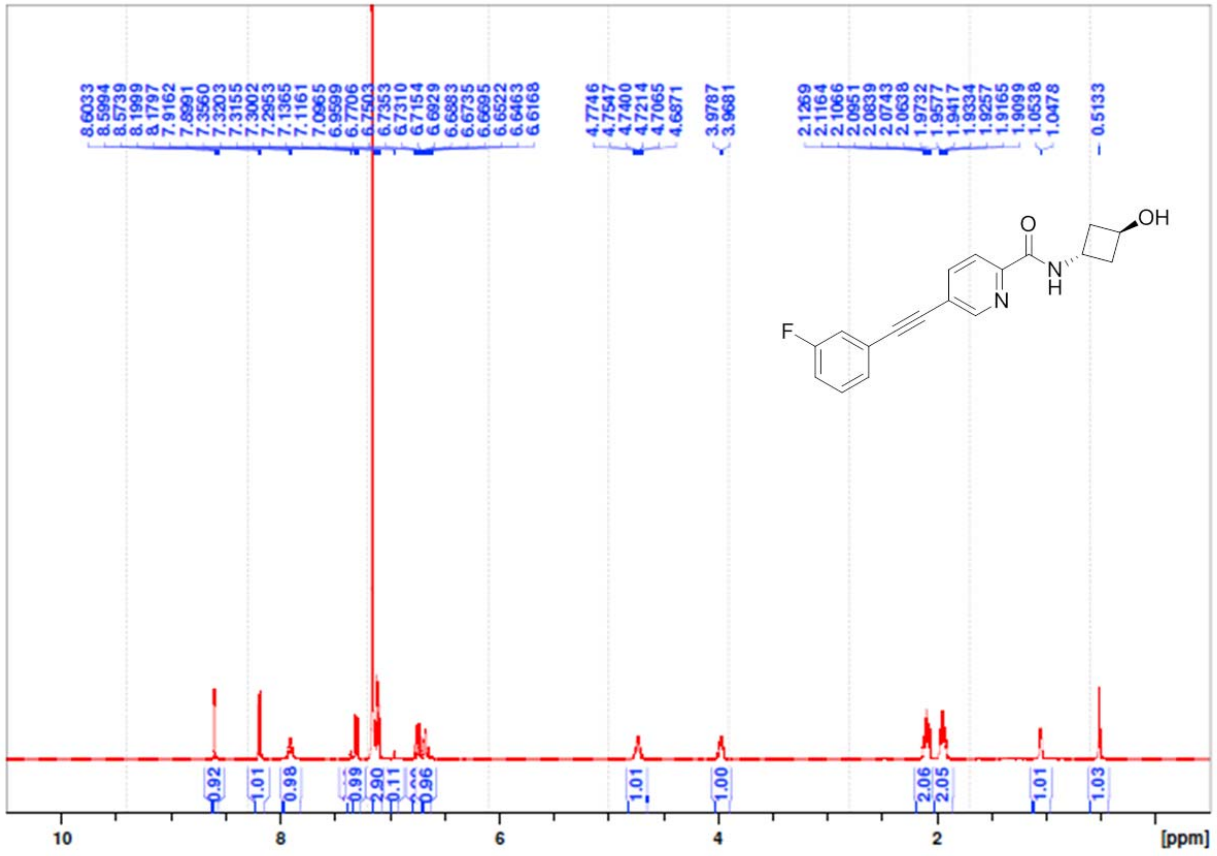

Figure S6. ^{1}H NMR of authentic standard VU0453103 (C6D6 at 500 MHz).

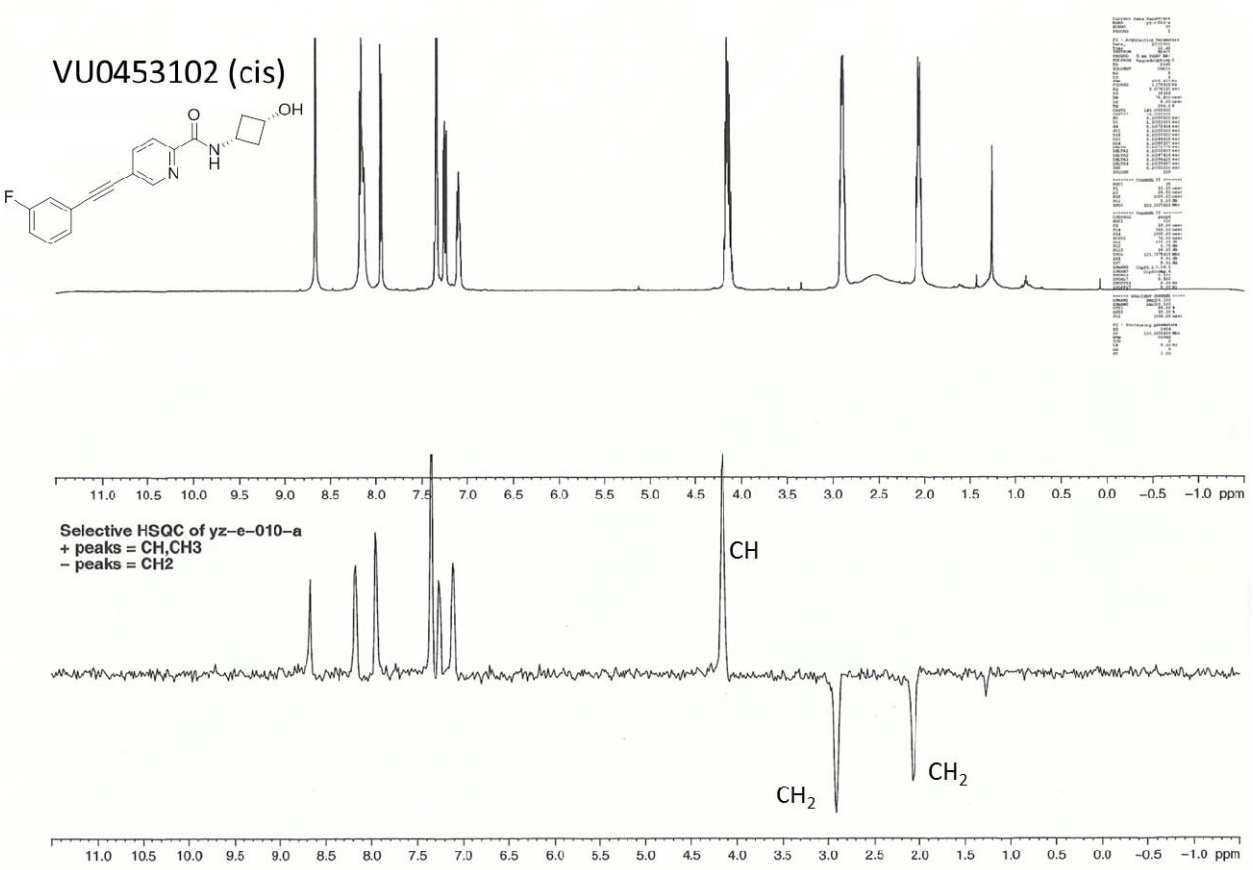

Figure S7. ^{1}H HSQC of authentic standard VU0453102 (peak A, cis) in CDCl3 at 500 MHz.

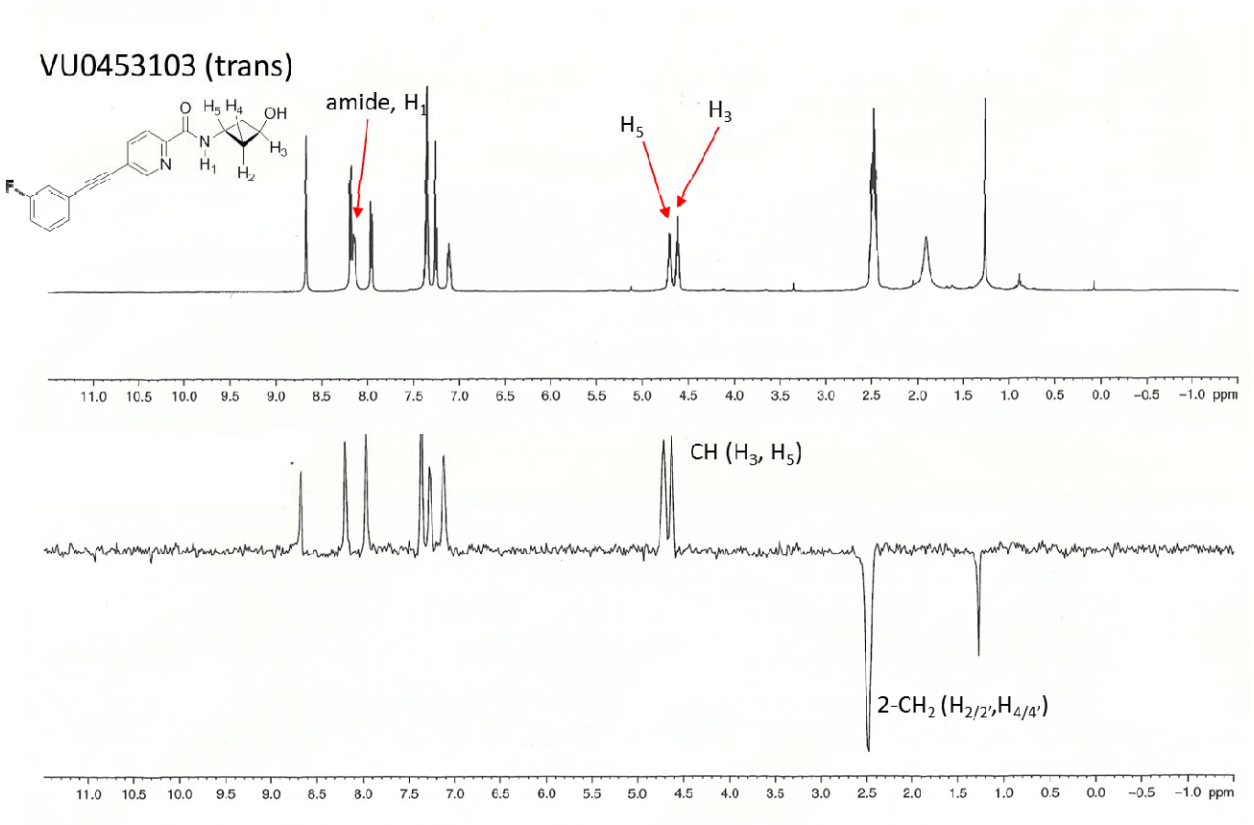

Figure S8. ^{1}H HSQC of authentic standard VU0453103 (peak B, trans) in CDCl3 at 500 MHz.

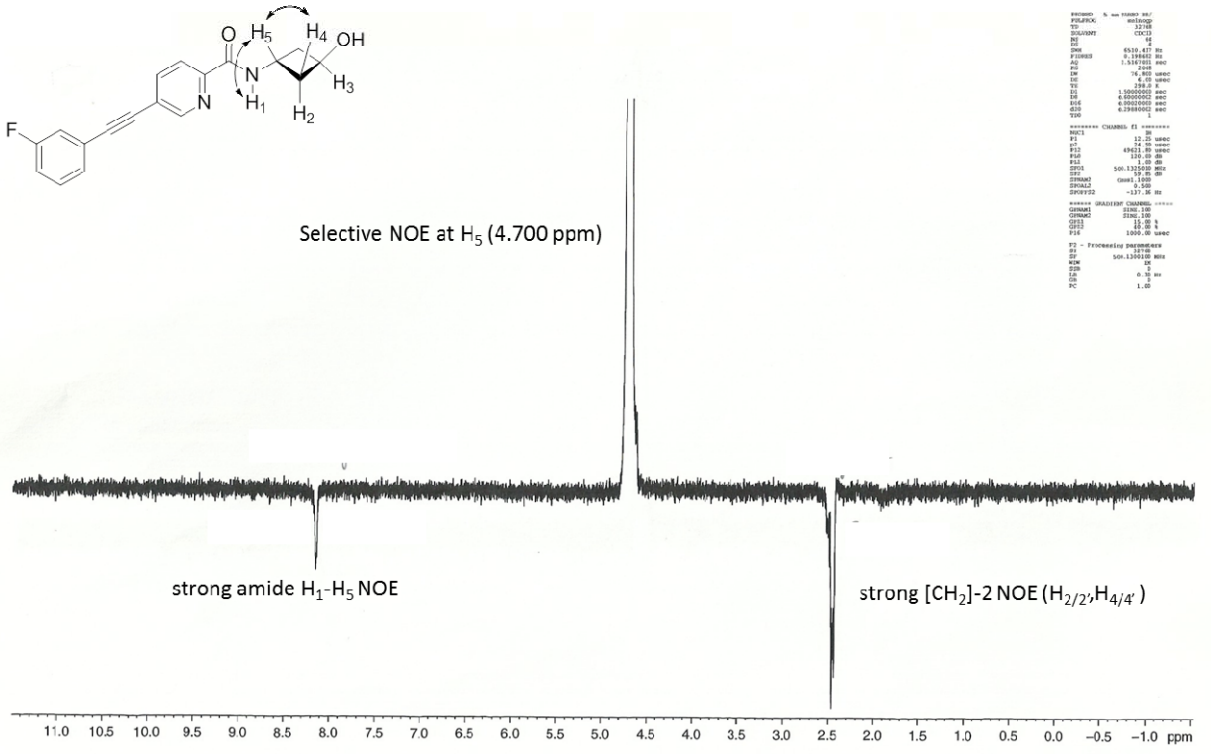

Figure S9. NOE of authentic standard VU0453103 (trans) in CDCl3 at 4.700 ppm (500 MHz).